5 Turbulence Kinetic Energy, Stability and Scaling

Turbulence kinetic energy (TKE) is one of the most important variables in micrometeorology, because it is a measure of the intensity of turbulence. It is directly related to the momentum, heat, and moisture transport through the boundary layer. Turbulence kinetic energy is also sometimes used as a starting point for approximations of turbulent diffusion.

The individual terms in the TKE budget equation describe physical processes that generate turbulence. The relative balance of these processes determines the ability of the flow to maintain turbulence or become turbulent, and thus indicates flow stability. Some important dimensionless groups and scaling parameters are also based on terms in the TKE equation. For these reasons, our study of turbulence kinetic energy will begin with the TKE budget equation, and end in a general discussion of stability and scaling.

5.1 The TKE Budget Derivation

The definition of TKE presented in section 2.5 is $TKE/m = \bar{e} = 0.5\,(\overline{u'^2} + \overline{v'^2} + \overline{w'^2})$.

Using summation notation, it is easy to rewrite this as $\bar{e} = 0.5\,\overline{u_i'^2}$. We recognize immediately that TKE/m is nothing more than the summed velocity variances divided by two. Therefore, starting with the prognostic equation for the sum of velocity variances (4.3.1g) and dividing by two easily gives us the TKE budget equation:

$$\frac{\partial \bar{e}}{\partial t} + \overline{U}_j \frac{\partial \bar{e}}{\partial x_j} = + \delta_{i3} \frac{g}{\overline{\theta}_v}\left(\overline{u_i'\theta_v'}\right) - \overline{u_i'u_j'} \frac{\partial \overline{U}_i}{\partial x_j} - \frac{\partial\left(\overline{u_j'e}\right)}{\partial x_j} - \frac{1}{\overline{\rho}} \frac{\partial\left(\overline{u_i'p'}\right)}{\partial x_i} - \varepsilon \tag{5.1a}$$

I II III IV V VI VII

Term I represents local ***storage*** or tendency of TKE.
Term II describes the ***advection*** of TKE by the mean wind.
Term III is the ***buoyant production or consumption term.*** It is a production or loss term depending on whether the heat flux $\overline{u_i'\theta_v'}$ is positive (during daytime over land) or negative (at night over land).
Term IV is a ***mechanical or shear production/loss term.*** The momentum flux $\overline{u_i'u_j'}$ is usually of opposite sign from the mean wind shear, because the momentum of the wind is usually lost downward to the ground. Thus, Term IV results in a positive contribution to TKE when multiplied by a negative sign.
Term V represents the ***turbulent transport*** of TKE. It describes how TKE is moved around by the turbulent eddies u_j'.
Term VI is a ***pressure correlation term*** that describes how TKE is redistributed by pressure perturbations. It is often associated with oscillations in the air (***buoyancy or gravity waves***).
Term VII represents the viscous ***dissipation*** of TKE; i.e., the conversion of TKE into heat.

If we choose a coordinate system aligned with the mean wind, assume horizontal homogeneity, and neglect subsidence, then a special form of the TKE budget equation can be written

$$\frac{\partial \bar{e}}{\partial t} = \frac{g}{\overline{\theta}_v}\left(\overline{w'\theta_v'}\right) - \overline{u'w'} \frac{\partial \overline{U}}{\partial z} - \frac{\partial\left(\overline{w'e}\right)}{\partial z} - \frac{1}{\overline{\rho}} \frac{\partial\left(\overline{w'p'}\right)}{\partial z} - \varepsilon \tag{5.1b}$$

I III IV V VI VII

Turbulence is ***dissipative***. Term VII is a loss term that always exists whenever TKE is nonzero. Physically, this means that turbulence will tend to decrease and disappear with time, unless it can be generated locally or transported in by mean, turbulent, or pressure processes. Thus, TKE is not a conserved quantity. The boundary layer can be turbulent only if there are specific physical processes generating the turbulence. In the next subsections, the role of each of the terms is examined in more detail.

5.2 Contributions to the TKE Budget

5.2.1 Term 1: Storage

Fig 2.10 shows that there can be substantial variation in the magnitude of TKE with time at any one height. Fig 5.1 shows a simulation of TKE over a two day period, where a dramatic increase and decrease of TKE occurs within each diurnal cycle. An increase in TKE from a small early morning value to a larger early afternoon value represents a net storage of TKE in the air. In particular, nonturbulent FA air just above the ML top must be ***spun up*** (i.e., its turbulence intensity must increase from near zero to the current ML value) as entrainment incorporates it into the ML.

Over a land surface experiencing a strong diurnal cycle, typical order of magnitudes for this term range from about 5×10^{-5} m^2 s^{-3} for surface-layer air over a 6 h interval, to about 5×10^{-3} m^2 s^{-3} for FA air that is spun up over 15 min (i.e., over a time interval corresponding to t_*). Fig 5.2 shows sample observations of TKE made in the surface layer, where TKE varies by about two orders of magnitude.

During the later afternoon and evening, a corresponding ***spin down*** (i.e., decrease of TKE with time) occurs where dissipation and other losses exceed the production of turbulence. The storage term is thus negative during this transition phase.

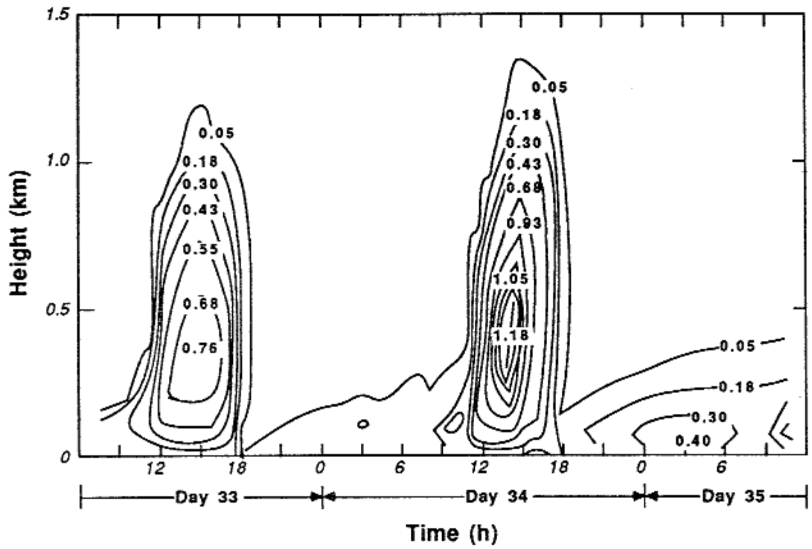

Fig. 5.1 Modeled time and space variation of $\bar{e}$ (turbulence kinetic energy, units m^{2}s^{-2}), for Wangara. From Yamada and Mellor (1975).

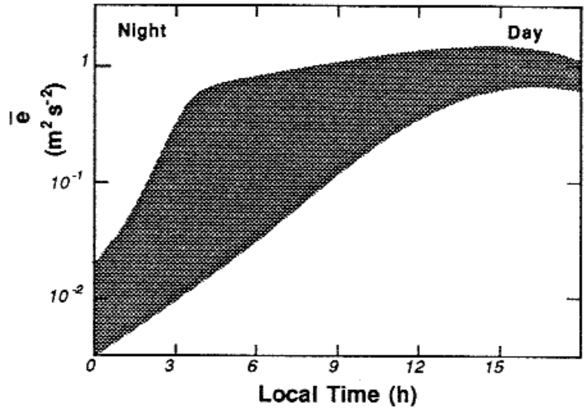

Fig. 5.2 Sample diurnal variation of observed range of turbulence kinetic energy, $\overline{e}$, in the surface layer during November. After Louis, et al. (1983).

Fig 5.3 indicates that the vertical profile of TKE can sometimes increase to a maximum at a height of about $z/z_i \cong 0.3$ when free convection dominates, as modeled for the Wangara experiment. When strong winds are present, the TKE might be nearly constant with height within the BL, or might decrease slightly with height as shown in Fig 5.3 for BLX83 data. At night, the TKE often decreases very rapidly with height, from a maximum value just above the surface.

Over surfaces such as oceans that do not experience a large diurnal cycle, the storage term is often so small that it can be neglected (i.e., steady state can be assumed). This is not to say that there is no turbulence, just that the intensity of turbulence is not changing significantly with time.

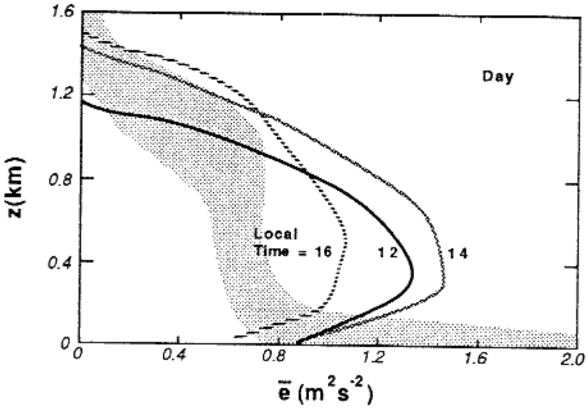

Fig. 5.3 The lines show modeled vertical profiles of turbulence kinetic energy, $\overline{e}$, during Day 33, Wangara, (after Therry and Lacarrere, 1983). The shaded profile applies when both shears and buoyancy are active (after Hechtel, 1988).

5.2.2 Term II: Advection

Little is known about this term. When averaged over a horizontal area larger than about 10 km by 10 km, it is often assumed that there is little horizontal variation in TKE, thereby making the advection term negligible. This is probably a good assumption over most land surfaces.

On a smaller scale, however, it is clear that this term must be important. For example, picture a reservoir of water cooler than the surrounding land. The lack of heating over the reservoir would allow turbulence to decay in the overlying air, while air over the adjacent land surfaces could be in a state of active convection. A mean wind advecting air across the shores of this reservoir would thus cause significant change in the TKE budget. Over ocean surfaces, the advection term would probably be negligible even on the small scales.

5.2.3 Term III: Buoyant Production/Consumption

Production. Fig 5.4 shows the variation of a number of TKE budget terms with height within a fair-weather convective ML. The most important part of the buoyancy term is the flux of virtual potential temperature, $\overline{w'\theta_v'}$. As we have already studied in

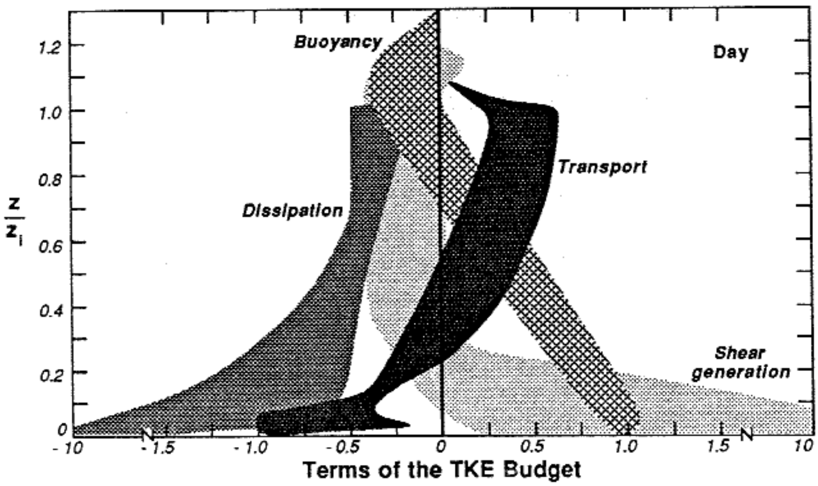

Fig. 5.4 Normalized terms in the turbulence kinetic energy equation. The shaded areas indicate ranges of values. All terms are divided by w_*^3 / z_i, which is on the order of $6\times 10^{-3} m^2 s^{-3}$. Based on data and models from Deardorff (1974), André et al. (1978), Therry and Lacarrere (1983), Lenschow (1974), Pennell and LeMone (1974), Zhou, et al. (1985) and Chou, et al. (1986).

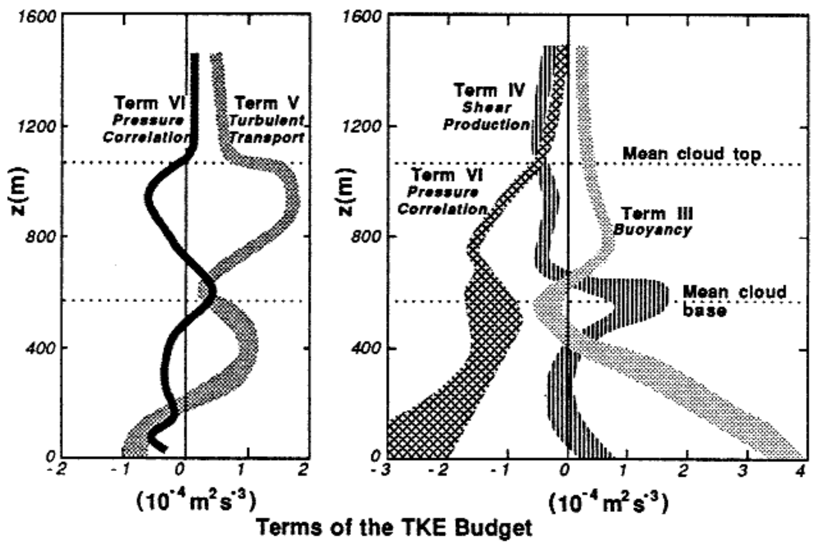

Fig. 5.5 Range of terms in the turbulent kinetic energy budget for a cloud - topped tropical boundary layer. The transport term is split into the pressure correlation (PC) and turbulent transport (T) parts. After Nicholls, et al. (1982).

the previous chapters, this flux is positive and decreases roughly linearly with height within the bottom 2/3 of the convective ML. Near the ground, term III is large and positive, corresponding to a large generation rate of turbulence whenever the underlying surface is warmer than the air.

When positive, this term represents the effects of ***thermals*** in the ML. Active thermal convection is associated with large values of this term, as large as $1 \times 10^{-2}\ m^2\ s^{-3}$ near the ground. Thus, we often associate this term with sunny days over land, or cold air advection over a warmer underlying surface. For cloudy days over land, it can be much smaller.

In convective boundary layers capped with actively growing cumulus clouds, the positive buoyancy within the cloud can contribute to the production (term III) of TKE (see Fig 5.5). Between this cloud layer contribution and the contribution near the bottom of the subcloud layer, there may be a region near cloud base where the air is statically stable and the buoyancy term is therefore negative.

Because Term III is so important on days of free convection, it is often used to normalize all the other terms. For example, using the definitions of w_* and z_i presented earlier, it is easy to show that Term III = $(w_*)^3 / z_i$ at the surface. Dividing (5.1b) by $(w_*)^3 / z_i$ gives a dimensionless form of the TKE budget equation that is useful for free convection situations:

$$\frac{z_i}{w_*^3}\frac{\partial \bar{e}}{\partial t} = \frac{g\, z_i \left(\overline{w'\theta_v'}\right)}{w_*^3\,\overline{\theta_v}} - \frac{z_i\,\overline{u'w'}}{w_*^3}\frac{\partial \overline{U}}{\partial z} - \frac{z_i}{w_*^3}\frac{\partial\left(\overline{w'e}\right)}{\partial z} - \frac{z_i}{w_*^3}\,\bar{\rho}\,\frac{\partial\left(\overline{w'p'}\right)}{\partial z} - \frac{z_i\,\varepsilon}{w_*^3} \qquad (5.2.3)$$

I III IV V VI VII

By definition, the dimensionless Term III is unity at the surface. Equations that are made dimensionless by dividing by scaling parameters are said to be ***normalized***. The normalization scheme expressed by (5.2.3) is used in most of the figures in this section, and indeed has been used in the previous chapter too.

As is evident in (4.3.1j), the buoyancy term acts only on the vertical component of TKE. Hence, this production term is ***anisotropic*** (i.e., not isotropic). The return-to-isotropy terms of (4.3.1h-j) are responsible for moving some of the vertical kinetic energy into the horizontal directions. Again, the anisotropic nature of Term III confirms our picture of strong up and downdrafts within thermals.

Consumption. In statically stable conditions, an air parcel displaced vertically by turbulence would experience a buoyancy force pushing it back towards its starting height. ***Static stability thereby tends to suppress, or consume, TKE***, and is

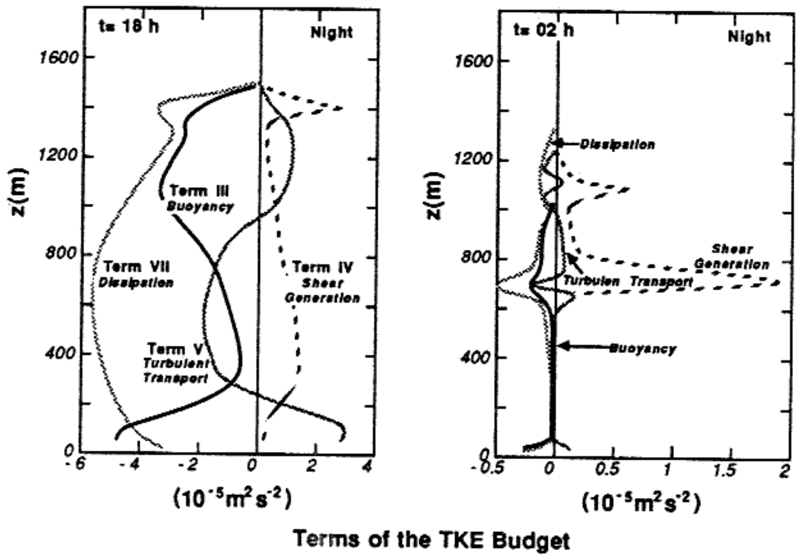

Fig. 5.6 Modeled turbulence kinetic energy budgets at t=18 h and t=02 h during Night 33-34, Wangara. After André et al. (1978).

associated with negative values of term III. Such conditions are present in the SBL at night over land, or anytime the surface is colder than the overlying air. An example of the decay of turbulence in negatively buoyant conditions just after sunset is shown in the budget profiles of Fig 5.6.

This same type of consumption can occur at the top of a ML, where warmer air entrained downward by turbulence opposes the descent because of its buoyancy (Stage and Businger, 1981). This is related to the negative values of the buoyancy term near the top of the ML in Fig 5.4.

5.2.4 Term IV: Mechanical (Shear) Production

When there is a turbulent momentum flux in the presence of a mean wind shear, the interaction between the two tends to generate more turbulence. Even though a negative sign precedes Term IV, the momentum flux is usually of opposite sign from the mean shear, resulting in production, not loss, of turbulence.

Fig. 5.4 shows case studies of the contribution of shear production to the TKE budget for convective situations. The greatest wind shear magnitude occurs at the surface. Not surprisingly, the maximum shear production rate also occurs there. As shown in Chapters 1 and 3, the wind speed frequently varies little with height in the ML above the surface layer, resulting in near zero shear and near zero shear production of turbulence. Shear production is often associated with the surface layer because of its limited vertical extent.

A smaller maximum of shear production sometimes occurs at the top of the ML because of the wind shear across the entrainment zone. In that region, the subgeostrophic winds of the ML recover to their geostrophic values above the ML.

The relative contributions of the buoyancy and shear terms can be used to classify the nature of convection (see Fig 5.7) ***Free convection*** scaling is valid when the buoyancy term is much larger than the mechanical term, ***forced convection*** scaling is valid when the opposite is true.

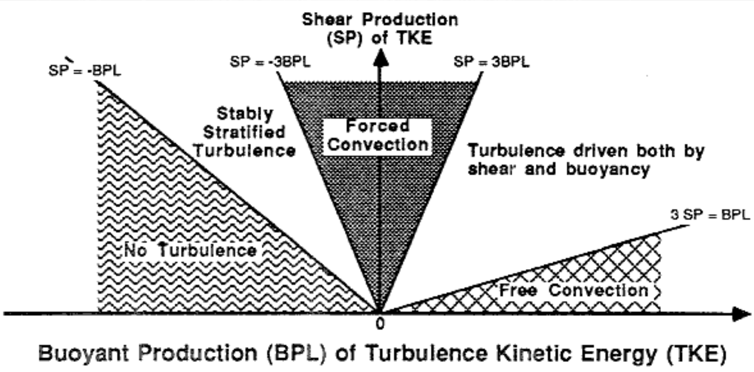

Fig. 5.7 Approximate regimes of free and forced convection.

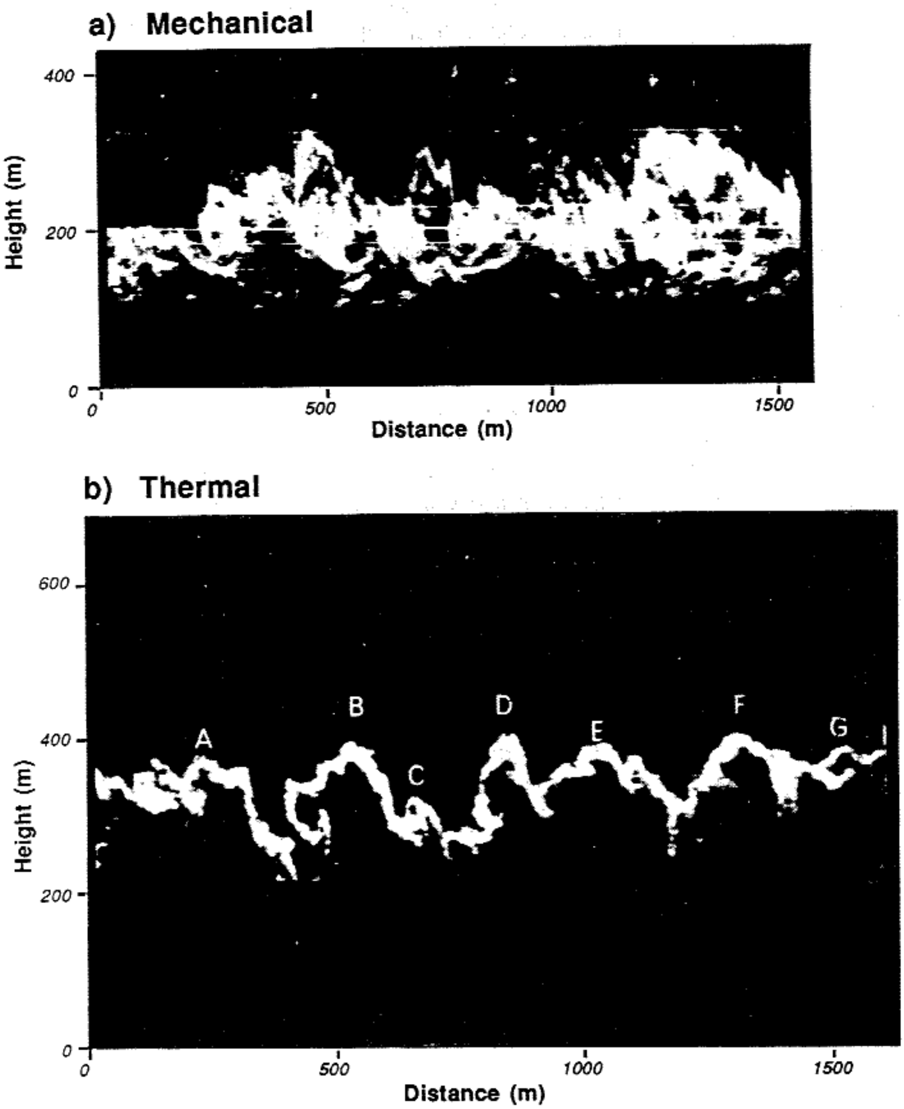

Fig. 5.8 Radar images of turbulence near the boundary layer top, showing (a) forced convection, and (b) free convection. After Noonkester (1974).

Magnitudes of the shear production term in the surface layer are obviously greatest on a windy day, and are small on a calm day. In synoptic-scale cyclones the strong winds and overcast skies suggest that forced convection is applicable. On many days, turbulence is neither in a state of free nor forced convection because both the shear and buoyancy terms are contributing to the production of turbulence.

At night over land, or anytime the ground is colder than the air, the shear term is often the only term that generates turbulence. We have seen from Fig 5.4 that the shear term is active over just a relatively small depth of air, so it is not surprising that, over land, the NBL is usually thinner than the ML.

The greatest shears are associated with the change of U and V components of mean wind with height. Except in thunderstorms, shear of W is negligible in the BL. Looking back on (4.3.1h-j), the shear production is greatest into the x and y components of TKE. Hence, shear production is also an anisotropic forcing — strongest in the horizontal.

Both the buoyant and shear production terms can generate anisotropic turbulence. The difference is that shear generation produces turbulence primarily in the horizontal directions, while buoyant generation produces it primarily in the vertical. These differences are evident in Fig. 5.8, where a high powered vertically pointing continuous-wave radar was used to observed the time evolution of eddy structure within the BL. This instrument senses moisture contrasts between dry and moist air. The boundary between regions of different moisture appear white in the photographs, while regions of more uniform high or low humidity appear black. Taylor's hypothesis has been used to convert from time-height graphs to vertical cross sections.

In Fig 5.8b for free convection, the "inverted U-shaped" tops of thermals shows up as white because they separate the dry FA air from the moister ML air. These structures are predominantly vertical. In Fig 5.8a for forced convection, the eddies are sheared into a much more horizontal or slanting orientation, with a much more chaotic appearance. Similar structures are apparent in the lidar-generated images shown in the frontispiece figure on page xiii, for (a) free and (b) forced convection.

5.2.5 Term V: Turbulent Transport

The quantity $\overline{w'e}$ represents the vertical turbulent flux of TKE. As for other vertical fluxes, the change in flux with height is more important than the magnitude of flux. Term V is a flux divergence term; if there is more flux into a layer than leaves, then the magnitude of TKE increases.

On a local scale (i.e., at any one height within the ML), Term V acts as either production or loss, depending on whether there is a flux convergence or divergence. When integrated over the depth of the ML, however, Term V becomes identically zero, assuming as bottom and top boundary conditions that the earth is not turbulent, and that there is negligible turbulence above the top of the ML. Overall, Term V neither creates nor destroys TKE, it just moves or redistributes TKE from one location in the BL to another.

Fig 5.9 shows vertical profiles of $\overline{w'e}$ for daytime, convective cases. Most of these

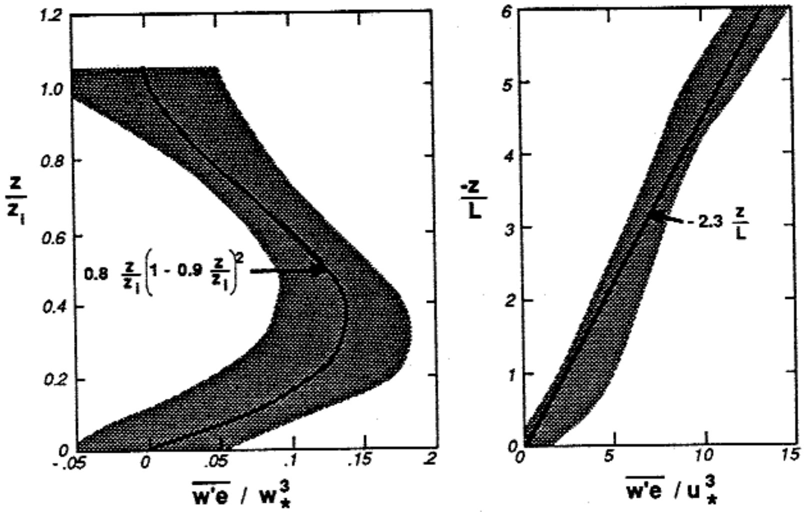

Fig. 5.9 Range of vertical profiles of the normalized vertical flux of turbulence kinetic energy using mixed layer scaling (left) and surface-layer scaling (right) where L is the Obukhov length. After Lenschow, et al. (1980), André, et al. (1978), Therry and Lacarrere (1983), and Pennell and LeMone (1974).

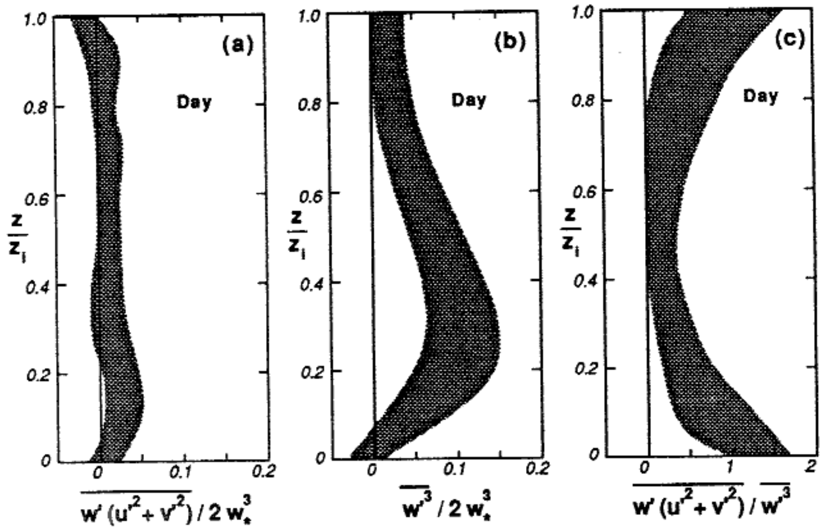

Fig. 5.10 (a) Range of vertical profiles of the normalized vertical flux of horizontal variance; (b), the vertical flux of vertical variance; (c), and the ratio of the two during daytime. After Lenschow, et al. (1980).

profiles show a maximum of $\overline{w'e}$ at $z/z_i = 0.3$ to 0.5. Below this maximum, there is more upward flux leaving the top of any one layer than enters from below, making a net divergence or loss of TKE. Above the maximum, there is a net convergence or production of TKE. The net effect is that some of the TKE produced near the ground is transported up to the top half of the ML before it is dissipated, as confirmed in Fig 5.4. Transport across the surface layer is illustrated in the right portion of Fig 5.9, where the Obukhov length L will be defined in section 5.7.

If one splits the vertical turbulent transport of total TKE into transport of w'^2 and $(u'^2+v'^2)$, then one finds that it is the vertical transport of w'^2 that dominates in the middle of the ML, and the transport of $(u'^2+v'^2)$ that dominates near the surface. Fig 5.10 shows these transports, as well as their ratio.

5.2.6 Term VI: Pressure Correlation

Turbulence. Static pressure fluctuations are exceedingly difficult to measure in the atmosphere. The magnitudes of these fluctuations are very small, being on the order of 0.005 kPa (0.05 mb) in the convective surface layer to 0.001 kPa (0.01 mb) or less in the ML. Pressure sensors with sufficient sensitivity to measure these static pressure fluctuations are contaminated by the large dynamic pressure fluctuations associated with turbulent and mean motions. As a result, correlations such as $\overline{w'p'}$ calculated from experimental data often contain more noise than signal.

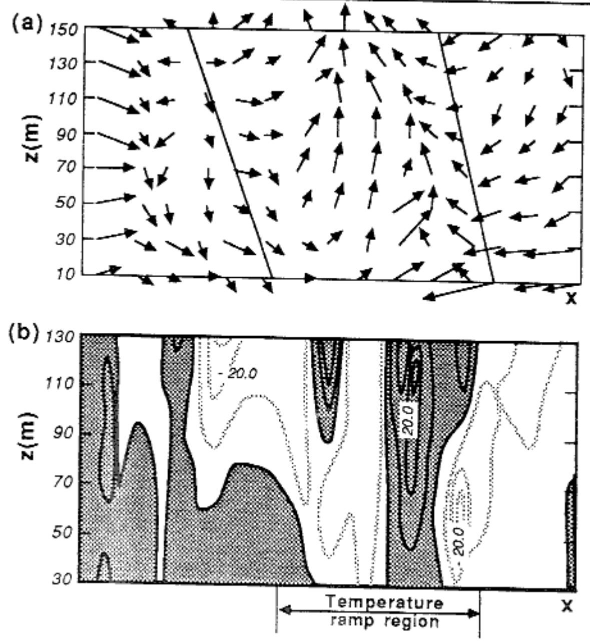

Fig. 5.11 (a) Composite of measured circulation patterns in a vertical cross-section thru convective thermals. Velocity vectors are deviations from the mean wind. Solid lines denote the boundaries of the temperature ramp associated with a thermal updraft; they are separated by a physical distance on the order of 100 m. (b) Contour x-z plot of $\overline{w'p'}/\rho u_*^3$, where the horizontal axis represents a composite of many thermals. Contour interval is 10.0. After Wilczak and Businger (1984).

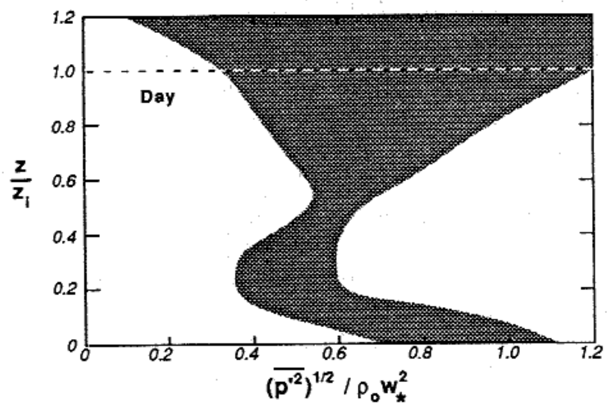

Fig. 5.12 Normalized Doppler- radar derived standard deviation of perturbation pressure. After Gal-chen and Kropfli (1984).

What little is known about the behavior of pressure correlation terms is estimated as a residual in the budget equations discussed previously. Namely, if all of the other terms in a budget equation are measured or parameterized, then the residual necessary to make the equation balance includes an estimate of the unknown term(s) together with the accumulated errors. An obvious hazard of this approach is that the accumulated errors from all of the other terms can be quite large.

Estimates of $\overline{w'p'}$ in the surface layer are shown in Fig 5.11 using this method, composited with respect to a large number of convective plume structures. We see quite a variation both in the vertical and horizontal. Here, the plume is defined by its temperature ramp signal. Fig 5.12 shows estimates of pressure variance based on Doppler radar measurements of motion within the ML.

Waves. Recall from chapters 1 and 2 that perturbations from a mean can describe waves as well as turbulence. Given measured values of $\overline{w'p'}$, it is impossible to separate the wave and turbulence contributions without additional information.

Work in linear gravity wave theory shows that $\overline{w'p'}$ is equal to the upward flux of wave energy for a vertically propagating internal gravity wave within a statically stable environment. This suggests that turbulence energy can be lost from the ML top in the form of internal gravity waves being excited by thermals penetrating the stable layer at the top of the ML. The amount of energy lost may be on the order of less than 10% of the total rate of TKE dissipation, but the resulting waves can sometimes enhance or trigger clouds.

Turbulence within stable NBLs can also be lost in the form of waves. One concludes that the pressure correlation term not only acts to redistribute TKE within the BL, but it can also drain energy out of the BL.

5.2.7 Term VII: Dissipation

As discussed in section 4.3.1, molecular destruction of turbulent motions is greatest for the smallest size eddies. The more intense this small-scale turbulence, the greater the rate of dissipation. Small-scale turbulence is, in turn, driven by the cascade of energy from the larger scales.

Daytime dissipation rates (see Fig 5.13) are often largest near the surface, and then become relatively constant with height in the ML. Above the ML top, the dissipation rate rapidly decreases to near zero. At night (see Fig 5.14), both TKE and dissipation rate decrease very rapidly with height. Because turbulence is not conserved, the greatest TKEs, and hence greatest dissipation rates, are frequently found where TKE production is the largest — near the surface. However, the dissipation rate is not expected to perfectly balance the production rate because of the various transport terms in the TKE budget.

Fig. 5.13
Range of normalized dissipation rate(ε) profiles during the daytime, where z_i is ML depth and w_* is the convective velocity scale. (After Caughey et al. (1979) and Kitchen et al. (1983)).

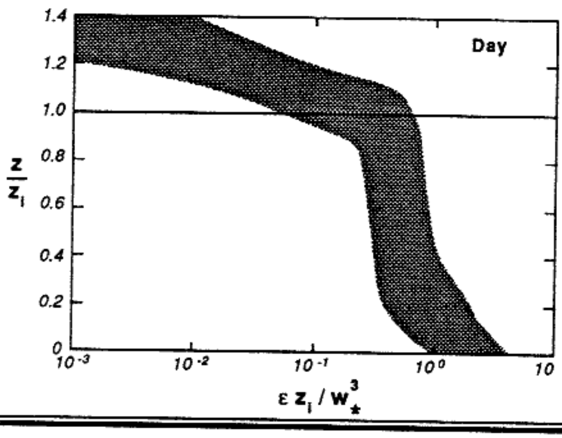

Fig. 5.14
Range of normalized dissipation rate(ε) profiles at night, where h is boundary layer depth and u_* is the friction velocity. After Caughey, et al. (1979).

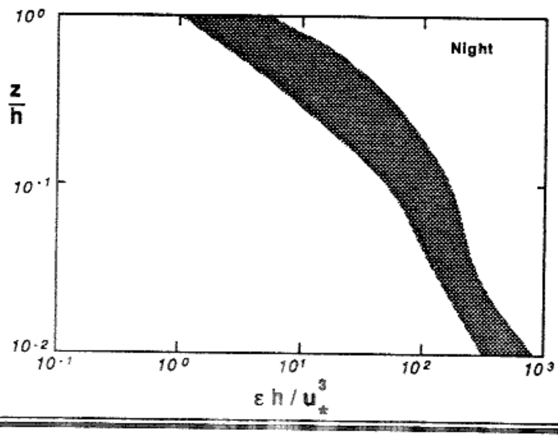

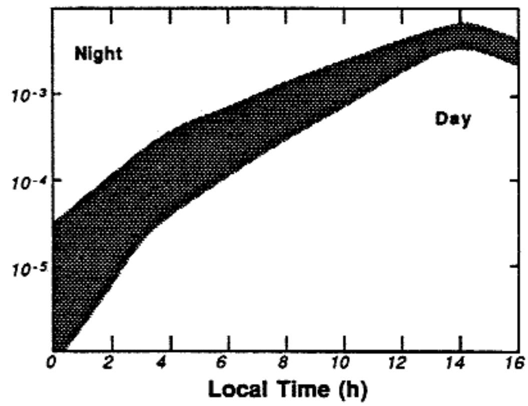

Fig. 5.15 Example of variation of dissipation rate with time from night to day. After Louis, et al. (1983).

The close relationship between TKE production rate, intensity of turbulence, and dissipation rate is shown in Fig 5.15. At night where only shear can produce turbulence, the dissipation rate is small because the associated TKE is small (refer back to Fig 5.2). After sunrise, buoyant production greatly increases the turbulence intensity, resulting in the associated increase in dissipation seen in Fig 5.15.

5.2.8 Example

Problem: At a height of z = 300 m in a 1000 m thick mixed layer the following conditions were observed: $\partial\overline{U}/\partial z = 0.01\ s^{-1}$, $\overline{\theta_v} = 25°C$, $\overline{w'\theta_v'} = 0.15$ K m/s, and $\overline{u'w'} = -0.03\ m^2s^{-2}$. Also, the surface virtual heat flux is 0.24 K m/s. If the pressure and turbulent transports are neglected, then (a) what dissipation rate is required to maintain a locally steady state at z = 300 m; and (b) what are the values of the normalized TKE terms?

Solution: (a) Since no information was given about the V-component of velocity or stress, let's assume that the x-axis has been chosen to be aligned with the mean wind. Looking at the TKE budget (5.1b), we know that term I must be zero for steady state, and terms V and VI are zero as specified in the statement of the problem. Thus, the remaining terms can be manipulated to solve for ε:

$$\varepsilon = \frac{g}{\overline{\theta_v}}\,\overline{w'\theta_v'} - \overline{u'w'}\,\frac{\partial\overline{U}}{\partial z}$$

Plugging in the values given above yields:

$$\varepsilon = \{(9.8\ \mathrm{m \cdot s^{-2}}) / [(273.15+25)\mathrm{K}]\} \cdot (0.15\ \mathrm{K \cdot m \cdot s^{-1}}) - (-0.03\ \mathrm{m^2 s^{-2}}) \cdot (0.01\ \mathrm{s^{-1}})$$

$$\varepsilon = 4.93 \times 10^{-3} + 3 \times 10^{-4}\ (\mathrm{m^2 s^{-3}})$$

$$\varepsilon = 5.23 \times 10^{-3}\ (\mathrm{m^2 s^{-3}})$$

(b) To normalize the equations as in (5.2.3), we first use (4.2a) to give $w_*^3 / z_i = (g/\overline{\theta_v}) \cdot \overline{w'\theta_v'}$, which for our case equals 7.89×10^{-3} ($\mathrm{m^2 s^{-3}}$). Dividing our terms by this value, and rewriting in the same order as (5.2.3) yields:

	0	=	0.625	+	0.038	-	0	-	0	-	0.663
Term:	I		III		IV		V		VI		VII

Discussion: This buoyant production term is about an order of magnitude larger than the mechanical production term, meaning that the turbulence is in a state of free convection. In regions of strong turbulence production, the transport term usually removes some of the TKE and deposits it where there is a net loss of TKE, such as in the entrainment zone. Thus, we might expect that the local dissipation rate at z = 300 m is smaller than the value calculated above.

5.3 TKE Budget Contributions as a Function of Eddy Size

As will be shown in chapter 8, the TKE budget equation can be written in a spectral form where the the contributions of each term in (5.1) can be examined as a function of wavelength or eddy size. Fig 5.16b shows the following terms as a function of wavenumber: buoyant production (Term III), shear production (Term IV), and dissipation (Term VII), all measured at one height in the BL. The turbulent transport and pressure redistribution term calculations were inaccurate, and hence left out of these figures.

One additional term appears in the spectral form of the TKE equation: the transfer of energy across the spectrum. In this case, as in most atmospheric cases, the transfer is from large size eddies (low wavenumbers) to small sizes (high wavenumbers). The concept behind this cascade of energy was introduced in Chapter 2. The rate of flow of this energy, shown in Fig 5.16a, is greatest for middle size eddies. Not only is it largest there, but it is also relatively constant with wavenumber. Hence, there is no net divergence or convergence of energy in the middle of the spectral domain, but there is a large amount of energy flowing through that domain. The slope of the curve in Fig 5.16a determines the magnitude of the transport term in Fig5.16b.

Large size eddies are presented on the left side of these figures, and small on the right. We see in Fig 5.16b that there is little energy at the very largest sizes, corresponding to the spectral gap. Once we get down to a normalized wavenumber of 0.01, we see large magnitudes of the shear and buoyant production terms. The production is not dissipated at these sizes however. Instead, there is the cascade or transport of energy away from the large size eddies towards the smaller sizes where it is deposited. At the small-eddy end of the spectrum (large wavenumber of 100-1000), the production terms are near zero. Instead, dissipation is large.

One measure of the smallest scales of turbulence is the Kolmogorov microscale, η, given by: $\eta = (\nu^3/\varepsilon)^{1/4}$. This scaling assumes that the smallest eddies see only turbulent energy cascading down the spectrum at rate ε, and feel only the viscous damping of ν. For the example of Fig 5.16, $\eta \cong 1$ mm, which occurs at a normalized frequency of about 3000.

The nature of the atmospheric turbulence spectrum is directly related to the fact that production and dissipation are not happening at the same scales. Production is feeding only the larger size eddies (anisotropically, as we learned earlier), but dissipation is acting only on the smaller sizes. Thus, the rate of transport across the middle part of the spectrum is equal to the rate of dissipation, ε, at the small-eddy end. Such transfer can be thought of as happening inertially — larger eddies creating or bumping into smaller ones, and transferring some of their inertia in the process. This middle portion of the spectrum is called the ***inertial subrange.***

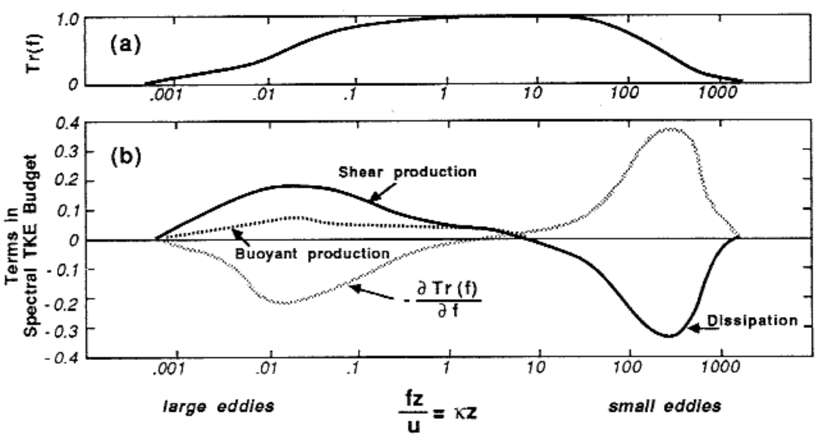

Fig. 5.16 Example of spectral energy budget terms for z/L = -0.29. Shown in (b) are the shear and buoyant production and the dissipation terms as functions of frequency f. The shaded curve (labelled $\partial Tr(f) / \partial f$) is equal to minus the sum of the shear, buoyant production and dissipation terms. The Tr(f) curve (a) was obtained by integrating $\partial Tr(f) / \partial f$. Here Tr(f) is the transfer of energy in f space required to balance the production and dissipation. The symbol f is frequency and κ is wave number. After McBean and Elliott (1975).

5.4 Mean Kinetic Energy and Its Interaction with Turbulence

Term IV in the TKE budget (5.1) involves the production of TKE by interaction of turbulence with the mean wind. One might expect that the production of TKE is accompanied by a corresponding loss of kinetic energy from the mean flow.

To study that possibility, start with the prognostic equation for mean wind in turbulent flow (3.4.3c), multiply by $\overline{U_i}$, and use the chain rule to derive the following equation for mean kinetic energy per unit mass [MKE/m = $0.5(\overline{U}^2 + \overline{V}^2 + \overline{W}^2) = 0.5\,\overline{U_i}^{\,2}$]:

$$\frac{\partial\left(0.5\overline{U_i}^{\,2}\right)}{\partial t} + \overline{U_j}\frac{\partial\left(0.5\,\overline{U_i}^{\,2}\right)}{\partial x_j} = -g\delta_{i3}\overline{U_i} + f_c\varepsilon_{ij3}\overline{U_i}\;\overline{U_j} - \frac{\overline{U_i}}{\overline{\rho}}\frac{\partial\overline{P}}{\partial x_i} + \nu\overline{U_i}\;\frac{\partial^2\overline{U_i}}{\partial x_j^2} - \overline{U_i}\frac{\partial\left(\overline{u_i'u_j'}\right)}{\partial x_j} \tag{5.4a}$$

I II III IV V VI X

- Term I represents storage of MKE.
- Term II describes the advection of MKE by the mean wind.
- Term III indicates that gravitational acceleration of vertical motions alter the MKE.
- Term IV shows the effects of the Coriolis force.
- Term V represents the production of MKE when pressure gradients accelerate the mean flow.
- Term VI represents the molecular dissipation of mean motions.
- Term X indicates the interaction between the mean flow and turbulence.

When the Coriolis term (IV) is summed over all values of the repeated indices, the result equals zero. This confirms our observation that Coriolis force can neither create nor destroy energy; it merely redirects the winds. Using the product rule, the last term (X) can be rewritten as

$$-\overline{U_i}\;\frac{\partial\left(\overline{u_i'u_j'}\right)}{\partial x_j} = \overline{u_i'u_j'}\;\frac{\partial\overline{U_i}}{\partial x_j} - \frac{\partial\left(\overline{u_i'u_j'}\;\overline{U_i}\right)}{\partial x_j}$$

This leaves

$$\frac{\partial\left(0.5\overline{U_i}^{\,2}\right)}{\partial t} + \overline{U_j}\frac{\partial\left(0.5\overline{U_i}^{\,2}\right)}{\partial x_j} = -g\overline{W} - \frac{\overline{U_i}}{\overline{\rho}}\frac{\partial\overline{P}}{\partial x_j} + \nu\,\overline{U_i}\;\frac{\partial^2\overline{U_i}}{\partial x_j^2} + \overline{u_i'u_j'}\;\frac{\partial\overline{U_i}}{\partial x_j} - \frac{\partial\left(\overline{u_i'u_j'}\;\overline{U_i}\right)}{\partial x_j} \tag{5.4b}$$

If we compare the TKE equation (5.1) with the MKE equation (5.4b):

$$\frac{\partial(\mathrm{TKE/m})}{\partial t} = \ldots - \overline{u_i'u_j'}\,\frac{\partial \overline{U_i}}{\partial x_j}$$

$$\frac{\partial(\mathrm{MKE/m})}{\partial t} = \ldots + \overline{u_i'u_j'}\,\frac{\partial \overline{U_i}}{\partial x_j}$$

we see that they both contain a term describing the interaction between the mean flow and turbulence. The sign of these terms differ. ***Thus, the energy that is mechanically produced as turbulence is lost from the mean flow***, and vice versa.

5.5 Stability Concepts

Unstable flows become or remain turbulent. Stable flows become or remain laminar. There are many factors that can cause laminar flow to become turbulent, and other factors that tend to stabilize flows. If the the net effect of all the destabilizing factors exceeds the net effect of the stabilizing factors, then turbulence will occur. In many cases, these factors can be interpreted as terms in the TKE budget equation.

To simplify the problem, investigators have historically paired one destabilizing factor with one stabilizing factor, and expressed these factors as a dimensionless ratio. Examples of these ratios are the Reynolds number, Richardson number, Rossby number, Froude number, and Rayleigh number. Some other stability parameters such as static stability, however, are not expressed in dimensionless form.

5.5.1 Static Stability and Convection

Static stability is a measure of the capability for buoyant convection. The word "static" means "having no motion"; hence this type of stability does not depend on wind. Air is statically unstable when less-dense air (warmer and/or moister) underlies more-dense air. The flow responds to this instability by supporting convective circulations such as thermals that allow buoyant air to rise to the top of the unstable layer, thereby stabilizing the fluid. Thermals also need some trigger mechanism to get them started. In the real boundary layer, there are so many triggers (hills, buildings, trees, dark fields, or other perturbations to the mean flow) that convection is usually insured, given the static instability.

Local Definitions. The traditional definition taught in basic meteorology classes is local in nature; namely, the static stability is determined by the local lapse rate. The local definition frequently fails in convective MLs, because the rise of thermals from near the surface or their descent from cloud top depends on their excess buoyancy and not on the ambient lapse rate.

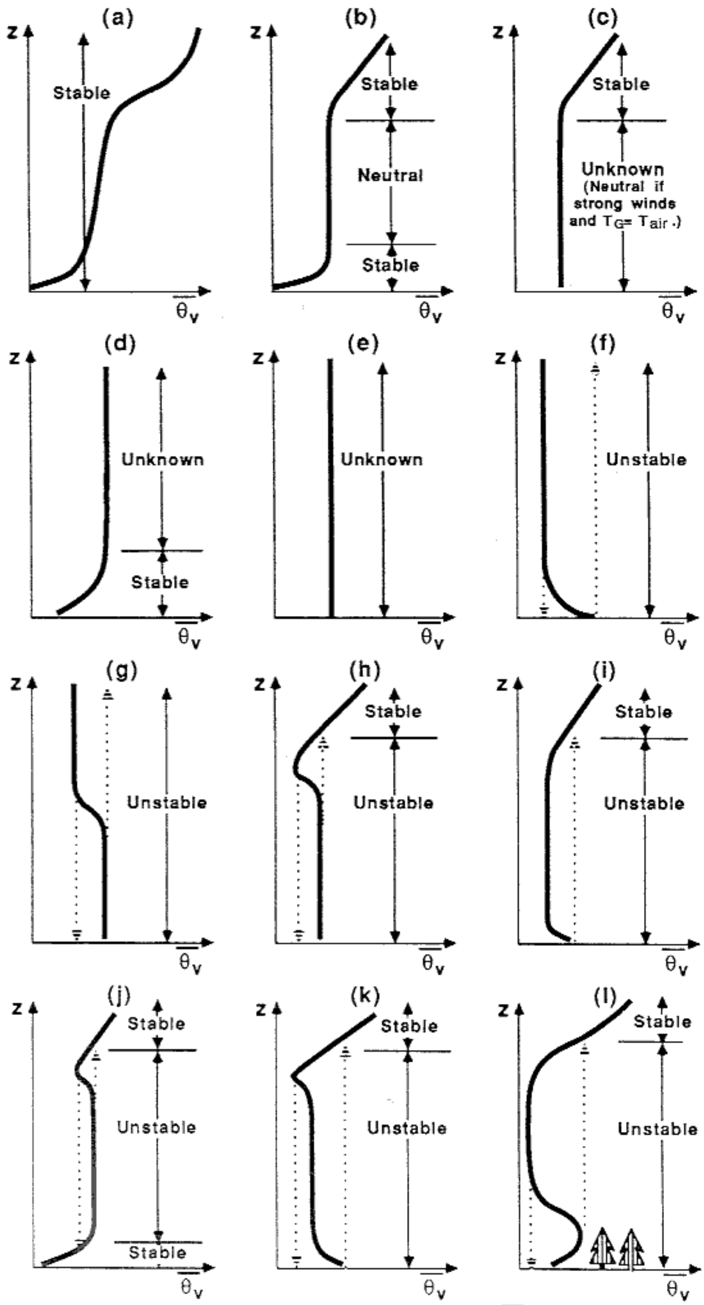

Fig. 5.17 Static stabilitiy as a function of the $\overline{\theta_v}$ profile. Dotted lines denote parcel movement.

As an example, in the middle 50% of the convective ML the lapse rate is nearly adiabatic, causing an incorrect classification of neutral stability if the traditional local definition is used. We must make a clear distinction between the phrases "adiabatic lapse rate" and "neutral stability". An ***adiabatic lapse rate*** (in the virtual potential temperature sense) may be statically stable, neutral, or unstable, depending on convection and the buoyancy flux. ***Neutral stability*** implies a very specific situation: adiabatic lapse rate AND no convection. The two phrases should NOT be used interchangeably, and the phrase "neutral lapse rate" should be avoided altogether.

We conclude that ***measurement of the local lapse rate alone is INSUFFICIENT to determine the static stability.*** Either knowledge of the whole $\overline{\theta_v}$ profile is needed (described next), or measurement of the turbulent buoyancy flux must be made.

Nonlocal Definitions. It is better to examine the stability of the whole layer, and make a layer determination of stability such as was done in section 1.6.4. For example, if $\overline{w'\theta_v'}$ at the earth's surface is positive, or if displaced air parcels will rise from the ground or sink from cloud top as thermals traveling across a BL, then the whole BL is said to be ***unstable*** or ***convective***. If $\overline{w'\theta_v'}$ is negative at the surface, or if displaced air parcels return to their starting point, then the BL is said to be ***stable***.

If, when integrated over the depth of the boundary layer, the mechanical production term in the TKE equation (5.1) is much larger than the buoyancy term, or if the buoyancy term is near zero, then the boundary layer is said to be ***neutral***. In some of the older literature, the boundary layer of this latter case is also sometimes referred to as an ***Ekman boundary layer***. During fair weather conditions over land, the BL touching the ground is rarely neutral. Neutral conditions are frequently found in the RL aloft. In overcast conditions with strong winds but little temperature difference between the air and the surface, the BL is often close to neutral stability.

In the absence of knowledge of convection or measurements of buoyancy flux, an alternate determination of static stability is possible if the $\overline{\theta_v}$ profile over the whole BL is known, as sketched in Fig 5.17. As is indicated in the figure, if only portions of the profile are known, then the stability might be indeterminate. Also, it is clear that there are many situations where the traditional local definition fails.

5.5.2 Example

Problem. Given the sounding at right, identify the static stability of the air at z = 600 m.

z (m)	$\overline{\theta_v}$(K)
1000	298
800	299
600	299
400	299
200	298
0	295

Solution. Using a local definition in the absence of heat fluxes, if we look downward from 600 m until a diabatic layer is encountered, we find a stable layer with cooler temperatures at 200 m. Before we reach any hasty conclusions, however, we must look up from 600 m. Doing so we find cooler unstable air at 1000 m. Thus, the static stability is unstable at 600 m.

Discussion. The whole adiabatic layer is unstable, considering the nonlocal approach of a cool parcel sinking from above. This sounding is characteristic of stratocumulus.

5.5.3 Dynamic Stability and Kelvin-Helmholtz Waves

The word "dynamic" refers to motion; hence, dynamic stability depends in part on the winds. Even if the air is statically stable, wind shears may be able to generate turbulence dynamically.

Some laboratory experiments have been performed (Thorpe, 1969, 1973; Woods 1969) using denser fluids underlying less-dense fluids with a velocity shear between the layers to simulate the stable stratification and shears of the atmosphere. Fig 5.18 is a sketch of the resulting flow behavior. The typical sequence of events is:

(1) A shear exists across a density interface. Initially, the flow is laminar.

(2) If a critical value of shear is reached (see section 5.6), then the flow becomes dynamically unstable, and gentle waves begin to form on the interface. The crests of these waves are normal to the shear direction

(3) These waves continue to grow in amplitude, eventually reaching a point where each wave begins to "roll up" or "break". This "breaking" wave is called a ***Kelvin-Helmholtz (KH) wave***, and is based on different physics than surface waves that "break" on an ocean beach.

(4) Within each wave, there exists some lighter fluid that has been rolled under denser fluid, resulting in patches of static instability. On radar, these features appear as braided ropelike patterns, "cat's eye" patterns or breaking wave patterns.

(5) The static instability, combined with the continued dynamic instability, causes each wave to become turbulent.

(6) The turbulence then spreads throughout the layer, causing a diffusion or mixing of the different fluids. During this diffusion process, some momentum is transferred between the fluids, reducing the shear between the layers. What was formerly a sharp, well-defined, interface becomes a broader, more diffuse shear layer with weaker shear and static stability.

(7) This mixing can reduce the shear below a critical value and eliminate the dynamic instability.
(8) In the absence of continued forcing to restore the shears, turbulence decays in the interface region, and the flow becomes laminar again.

This sequence of events is suspected to occur during the onset of ***clear air turbulence (CAT)***. These often occur above and below strong wind jets, such as the nocturnal jet and the planetary-scale jet stream. In these situations, however, continued dynamic forcings can allow turbulence to continue for hours to days. These regions of CAT have large horizontal extent (hundreds of kilometers in some cases), but usually limited vertical extent (tens to hundred of meters). They can be visualized as large pancake-shaped regions of turbulence. Aircraft encountering CAT can often climb or descend into smoother air.

Although KH waves are probably a frequent occurrence within statically stable shear layers, they are only rarely observed with the naked eye. Occasionally, there is sufficient moisture in the atmosphere to allow cloud droplets to act as visible tracers. Clouds that form in the rising portions of the waves often form parallel bands called ***billow clouds***. The orientation of these bands is perpendicular to the shear vector. One must remember that the wind SHEAR vector need not necessarily point in the same direction as the mean wind vector.

For both static and dynamic instabilities, and many other instabilities for that matter, it is interesting to note that the fluid reacts in a manner to undo the cause of the instability. This process is strikingly similar to ***LeChatelier's principle*** of chemistry, which states that "if some stress is brought to bear upon a system in equilibrium, a change occurs such that the equilibrium is displaced in a direction which tends to undo the effect of the stress". Thus, turbulence is a mechanism whereby fluid flows tend to undo the cause of the instability. In the case of static instabilities, convection occurs that tends to move more buoyant fluid upward, thereby stabilizing the system. For dynamic instability, turbulence tends to reduce the wind shears, also stabilizing the system.

With this in mind, it is apparent that turbulence acts to eliminate itself. After the unstable system has been stabilized, turbulence tends to decay. Given observations of turbulence occurring for long periods of time within the boundary layer, it is logical to surmise that there must be external forcings tending to destabilize the BL over long time periods. In the case of static instability, the solar heating of the ground by the sun is that external forcing. In the case of dynamic instabilities, pressure gradients imposed by synoptic-scale features drive the winds against the dissipative effects of turbulence.

By comparing the relative magnitudes of the shear production and buoyant consumption terms of the TKE equation, we can hope to estimate when the flow might become dynamically unstable. The Richardson number, Ri, described in the next subsection, can be used as just such an indicator.

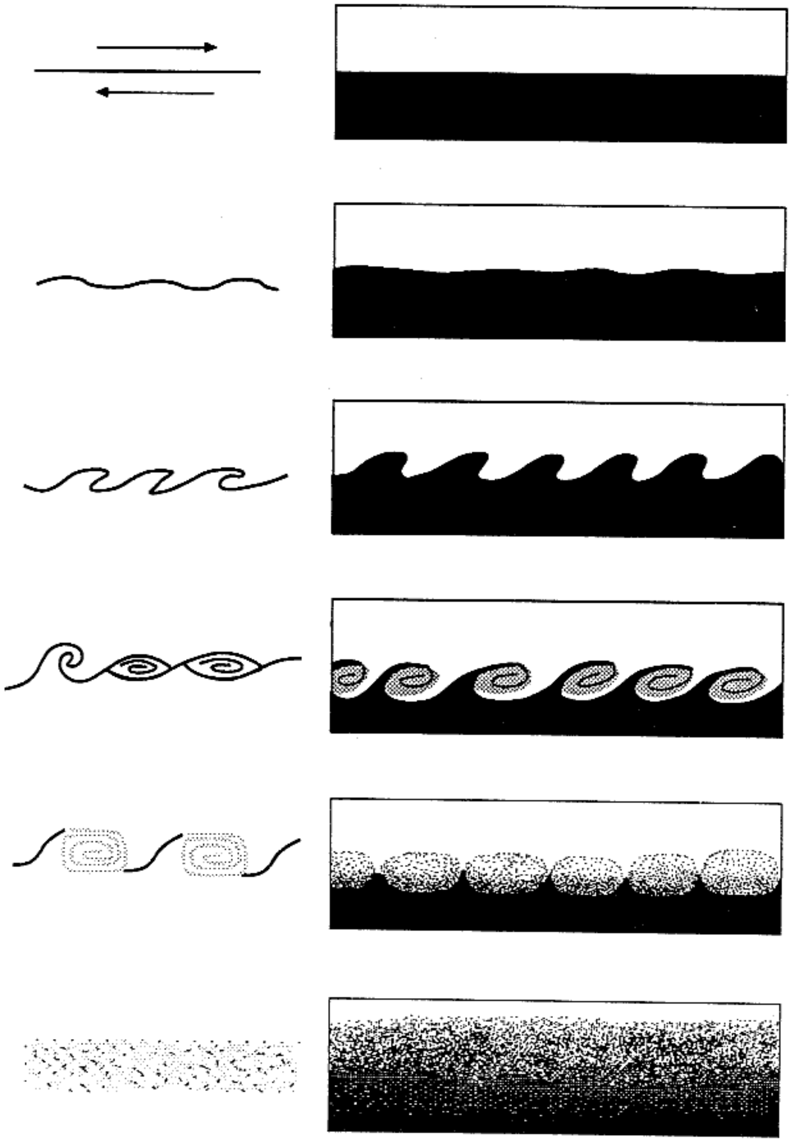

Fig. 5.18 Schematic diagram of Kelvin-Helmholtz instability in a laboratory experiment where shear flow has been generated. The upper layer, water, flows to the right, and the lower more dense fluid, dyed brine, flows to the left. The figures are about half a second apart. After Thorpe (1969,1973) and Woods (1969).

5.6 The Richardson Number

5.6.1 Flux Richardson Number

In a statically stable environment, turbulent vertical motions are acting against the restoring force of gravity. Thus, buoyancy tends to suppress turbulence, while wind shears tend to generate turbulence mechanically. The buoyant production term (Term III) of the TKE budget equation (5.1b) is negative in this situation, while the mechanical production term (Term IV) is positive. Although the other terms in the TKE budget are certainly important, a simplified but nevertheless useful approximation to the physics is possible by examining the ratio of Term III to Term IV. This ratio, called the ***flux Richardson number***, R_f, is given by

$$R_f = \frac{\left(\frac{g}{\overline{\theta_v}}\right)\overline{(w'\theta_v')}}{\overline{(u_i'u_j')}\frac{\partial \overline{U_i}}{\partial x_j}} \qquad (5.6.1a)$$

where the negative sign on Term IV is dropped by convention. The Richardson number is dimensionless. The denominator consists of 9 terms, as implied by the summation notation.

If we assume horizontal homogeneity and neglect subsidence, then the above equation reduces to the more common form of the flux Richardson number:

$$R_f = \frac{\left(\frac{g}{\overline{\theta_v}}\right)\overline{(w'\theta_v')}}{\overline{(u'w')}\frac{\partial \overline{U}}{\partial z} + \overline{(v'w')}\frac{\partial \overline{V}}{\partial z}} \qquad (5.6.1b)$$

For statically unstable flows, R_f is usually negative (remember that the denominator is usually negative). For neutral flows, it is zero. For statically stable flows, R_f is positive.

Richardson proposed that $R_f = +1$ is a critical value, because the mechanical production rate balances the buoyant consumption of TKE. At any value of R_f less than +1, static stability is insufficiently strong to prevent the mechanical generation of turbulence. For negative values of R_f, the numerator even contributes to the generation of turbulence. Therefore, he expected that

Flow IS turbulent (dynamically unstable) when $R_f < +1$

Flow BECOMES laminar (dynamically stable) when $R_f > +1$

We recognize that statically unstable flow is, by definition, always dynamically unstable.

5.6.2 Gradient Richardson Number

A peculiar problem arises in the use of R_f ; namely, we can calculate its value only for turbulent flow because it contains factors involving turbulent correlations like $\overline{w'\theta_v'}$. In other words, we can use it to determine whether turbulent flow will become laminar, but not whether laminar flow will become turbulent.

Using the reasoning of section 2.7 and Fig 2.13, it is logical to suggest that the value of the turbulent correlation $-\overline{w'\theta_v'}$ might be proportional to the lapse rate $\partial\overline{\theta_v}/\partial z$. Similarly, we might suggest that $-\overline{u'w'}$ is proportional to $\partial\overline{U}/\partial z$, and that $-\overline{v'w'}$ is proportional to $\partial\overline{V}/\partial z$. These arguments form the basis of a theory known as K-theory or eddy diffusivity theory, which will be discussed in much more detail in chapter 6. For now, we will just assume that the proportionalities are possible, and substitute those in (5.6.1b) to give a new ratio called the ***gradient Richardson number***, Ri :

$$\mathrm{Ri} = \frac{\dfrac{g}{\overline{\theta_v}}\dfrac{\partial\overline{\theta_v}}{\partial z}}{\left[\left(\dfrac{\partial\overline{U}}{\partial z}\right)^2 + \left(\dfrac{\partial\overline{V}}{\partial z}\right)^2\right]} \qquad (5.6.2)$$

When investigators refer to a "Richardson number" without specifying which one, they usually mean the gradient Richardson number.

Theoretical and laboratory research suggest that laminar flow becomes unstable to KH-wave formation and the ONSET of turbulence when Ri is smaller than the ***critical Richardson number***, R_c . Another value, R_T, indicates the termination of turbulence. The dynamic stability criteria can be stated as follows:

Laminar flow becomes turbulent when $\mathrm{Ri} < R_c$.

Turbulent flow becomes laminar when $\mathrm{Ri} > R_T$.

Although there is still some debate on the correct values of R_c and R_T, it appears that R_c = 0.21 to 0.25 and R_T = 1.0 work fairly well. Thus, there appears to be a ***hysteresis*** effect because R_T is greater than R_c.

One hypothesis for the apparent hysteresis is as follows. Two conditions are needed for turbulence: instability, and some trigger mechanism. Suppose that dynamic instability occurs whenever $\mathrm{Ri} < R_T$. If one trigger mechanism is existing turbulence in or adjacent to the unstable fluid, then turbulence can continue as long as $\mathrm{Ri} < R_T$ because of the presence of both the instability and the trigger. If KH waves are another trigger mechanism, then in the absence of existing turbulence one finds that Ri must get well below R_T before KH waves can form. Laboratory and theoretical work have shown that the criterion for KH wave formation is $Ri < R_c$. This leads to the apparent hysteresis, because the Richardson number of nonturbulent flow must be lowered to R_c before turbulence will start, but once turbulent, the turbulence can continue until the Richardson number is raised above R_T.

5.6.3 Bulk Richardson Number

The theoretical work yielding $R_c \cong 0.25$ is based on local measurements of the wind shear and temperature gradient. Meteorologists rarely know the actual local gradients, but can approximate the gradients using observations made at a series of discrete height intervals. If we approximate $\partial\overline{\theta_v}/\partial z$ by $\Delta\overline{\theta_v}/\Delta z$, and approximate $\partial\overline{U}/\partial z$ and $\partial\overline{V}/\partial z$ by $\Delta\overline{U}/\Delta z$ and $\Delta\overline{V}/\Delta z$ respectively, then we can define a new ratio known as the ***bulk Richardson number***, R_B :

$$R_B = \frac{g \, \Delta\overline{\theta_v} \, \Delta z}{\overline{\theta_v} \, [(\Delta\overline{U})^2 + (\Delta\overline{V})^2]} \qquad (5.6.3)$$

It is this form of the Richardson number that is used most frequently in meteorology, because rawinsonde data and numerical weather forecasts supply wind and temperature measurements at discrete points in space. The sign of the finite differences are defined, for example, by $\Delta\overline{U} = \overline{U}(z_{top}) - \overline{U}(z_{bottom})$.

Unfortunately, the critical value of 0.25 applies only for local gradients, not for finite differences across thick layers. In fact, the thicker the layer is, the more likely we are to average out large gradients that occur within small subregions of the layer of interest. The net result is (1) we introduce uncertainty into our prediction of the occurrence of turbulence, and (2) we must use an artificially large (theoretically unjustified) value of the critical Richardson number that gives reasonable results using our smoothed gradients. The thinner the layer, the closer the critical Richardson number will likely be to 0.25. Since data points in soundings are sometimes spaced far apart in the vertical, approximations such as shown in the graph and table in Fig 5.19 can be used to estimate the probability and intensity of turbulence (Lee, et al., 1979).

Table 5-1 shows a portion of a rawinsonde sounding, together with the corresponding values of bulk Richardson number. The resulting turbulence diagnosis is given in the rightmost column of Table 5-1. Note that the Richardson number itself says nothing about the intensity of turbulence, only about the yes/no presence of turbulence.

Fig. 5.19
(a) Relationship between the bulk Richardson number, Ri, over a layer and the probability of turbulence within that layer. This curve was developed empirically. (b) Empirically derived relationship between turbulence intensity and the wind speed and shear. "N" indicates none, "L" is light, "M" is moderate, "S" is severe, and "X" is extreme turbulence.

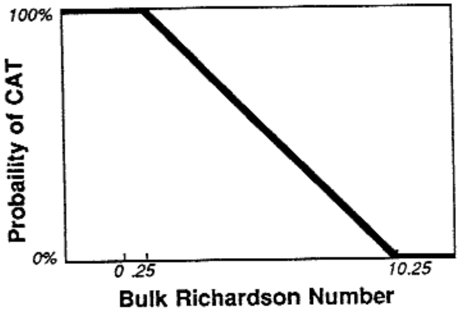

Wind Speed m/s (kt)	Vector wind shear s⁻¹ (kt/1000 feet) .0084-.0118 (5-7)	.0118-.0169 (7-10)	.0169-.0338 (10-20)	.0338-.0506 (20-30)	.0506-.0844 (30-50)	.0844+ (50+)
20-30 (40-60)	N	L	L-M	M	M-S	S
30-60 (60-120)	L	L-M	M	M-S	S	S-X
60+ (120+)	L	L-M	M	M-S	S	X

Fig 5.20 show examples of the evolution of the Richardson number during some nighttime case studies. Regions where the Richardson number is small are sometimes used as an indicator of the depth of the turbulent SBL. Here we see low Richardson numbers close to the ground, in addition to patches of low Richardson number aloft.

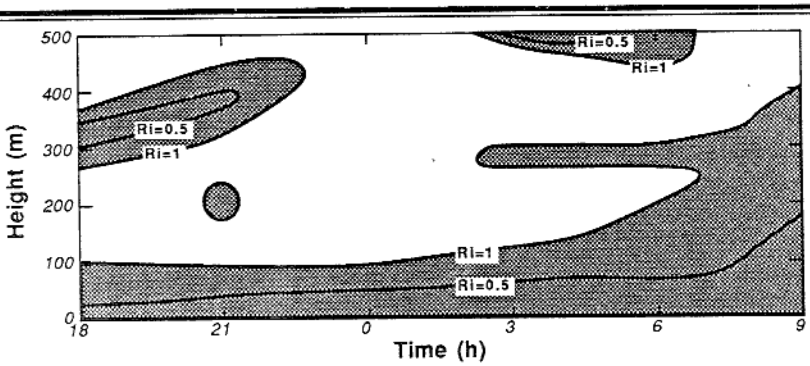

Fig. 5.20 Example of the evolution of local Richardson number with height and time during one night. Regions with Richardson number less than 1.0 are shaded, and are likely to be turbulent. After Mahrt (1981).

Table 5-1. Example of a nighttime rawinsonde sounding analyzed to give stability, shear, Richardson number, and the probability and intensity of turbulence. Probabilities are expressed as a percent, and intensities are abbreviated by:

N = no turbulence, L = light (0.5 G), M = moderate (1 G), S=severe (2 G)

These intensity levels correspond to the turbulence reporting recommendations used in aviation, where the vertical acceleration measured in Gs (number of times the pull of gravity) is relative to the center of gravity of the aircraft. For practical purposes, a probability greater than 50% AND an intensity greater than L were required before a CAT forecast would be issued.

z (m)	Wind Dir (°)	Speed (m/s)	T (K)	θ (K)	Lapse (K/m)	Shear (s^{-1})	R_B	CAT Prob(%)	CAT Inten.
1591	154	9.8	281	294.4	0.0021	0.0034	6.19	41	N
1219	150	10.7	-	-	0.0021	0.0045	3.43	68	N
914	144	9.7	-	-	0.0021	0.0091	0.86	94	N-L
702	-	-	287.8	292.5	0.0020	0.0091	0.81	94	N-L
610	134	7.4	-	-	0.0020	0.0170	0.23	100	L-M
393	-	-	290.2	291.9	0.0204	0.0170	2.37	79	L-M
305	95	3.5	-	-	0.0204	0.0137	3.64	66	N
222	79	2.7	288.4	288.4	0.0133	0.0071	8.92	13	N
4	45	2.5	287.6	285.5	-	-	-	-	-

5.6.4 Examples

Problem A: Given the same data from problem 5.2.8, calculate the flux Richardson number and comment on the dynamic stability.

Solution. Since the flux Richardson number is defined as the ratio of the buoyancy term to the negative of the shear term, we can use the values for these terms already calculated in example 5.2.8:

$$R_f = \frac{\text{buoyancy term}}{\text{- shear term}} = \frac{0.00493}{-0.0003} = -16.4$$

Discussion. A negative Richardson number is without question less than +1, and thus indicates dynamic instability and turbulence. This is a trivial conclusion, because any flow that is statically unstable is also dynamically unstable by definition.

Problem B: Given a fictitious SBL where $(g/\overline{\theta_v}) = 0.033\ m\ s^{-2}\ K^{-1}$, $\partial\overline{U}/\partial z = [u_* / (0.4 \cdot z)]\ s^{-1}$, $u_* = 0.4$ m/s, and where the lapse rate, c_1, is constant with height such that there is 6°C $\overline{\theta_v}$ increase with each 200 m of altitude gained. How deep is the turbulence?

Solution. We can use the gradient Richardson number as an indicator of dynamic stability and turbulence. Using the prescribed gradients, we find that:

$$Ri = \frac{\frac{g}{\overline{\theta_v}} \frac{\partial \overline{\theta_v}}{\partial z}}{\left(\frac{\partial \overline{U}}{\partial z}\right)^2} = \frac{\frac{g}{\overline{\theta_v}} c_1}{\left(\frac{u_*}{0.4z}\right)^2} = \frac{(0.033)\cdot(0.03)}{(0.4 / 0.4)^2} z^2 = (0.00099\ m^{-2})\ z^2$$

If we use $R_c = 0.25$, then we can use this critical value in place of Ri above and solve for z at the critical height above which there is no turbulence:

$$z = \sqrt{(1010\ m^2)\ R_c} = \sqrt{252.5\ m^2} = 15.9\ m$$

Discussion. If we has used a critical termination value of $R_T = 1.0$, then we would have found a critical height of 31.8 m. Thus, below 15.9 m we expect turbulence, while above 31.8 m we expect laminar flow. Between these heights the turbulent state depends on the past history of the flow at that height. If previously turbulent, it is turbulent now.

5.7 The Obukhov Length

The Obukhov length (L) is a scaling parameter that is useful in the surface layer. To show how this parameter is related to the TKE equation, first recall that one definition of the surface layer is that region where turbulent fluxes vary by less that 10% of their magnitude with height. By making the constant flux (with height) approximation, one can use surface values of heat and momentum flux to define turbulence scales and nondimensionalize the TKE equation.

Start with the TKE equation (5.1a), multiply the whole equation by $(-k\ z/u_*^3)$, assume all turbulent fluxes equal their respective surface values, and focus on just terms III, IV, and VII:

$$\ldots = -\frac{k\,z\,g\,(\overline{w'\theta_v'})_s}{\overline{\theta_v}\,u_*^3} + \frac{k\,z\,(\overline{u_i'u_j'})_s}{u_*^3}\frac{\partial \overline{U_i}}{\partial x_j} + \ldots - \frac{k\,z\,\varepsilon|_s}{u_*^3} \qquad (5.7a)$$

III IV VII

Each of these terms is now dimensionless. The last term, a dimensionless dissipation rate, will not be pursued further here.

The ***von Karman constant***, k, is a dimensionless number included by tradition. Its importance in the log wind profile in the surface layer is discussed in the next section. Investigators have yet to pin down its precise value, although preliminary experiments suggest that it is between about 0.35 and 0.42 . We will use a value of 0.4 in most of this book, although some of the figures adopted from the literature are based on k=0.35.

Term III is usually assigned the symbol, ζ, and is further defined as $\zeta \equiv z/L$, where L is the ***Obukhov length***. Thus,

$$\zeta = \frac{z}{L} = \frac{-k\, z\, g\, (\overline{w'\theta_v'})_s}{\overline{\theta_v}\, u_*^3} \tag{5.7b}$$

The Obukhov length is given by:

$$L = \frac{-\overline{\theta_v}\, u_*^3}{k\, g\, (\overline{w'\theta_v'})_s} \tag{5.7c}$$

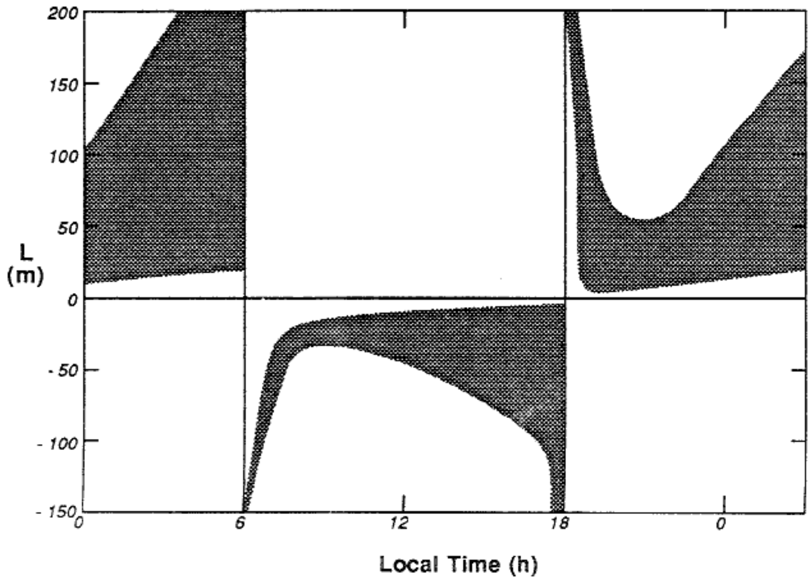

Fig. 5.21 Typical ranges of Obukhov length (L) evolution over a diurnal cycle.

One physical interpretation of the Obukhov length is that it is proportional to the height above the surface at which buoyant factors first dominate over mechanical (shear) production of turbulence. For convective situations, buoyant and shear production terms are approximately equal at $z = -0.5\,L$. Fig 5.21 shows the typical range of variations of the Obukhov length in fair weather conditions over land.

The parameter ζ turns out to be very important for scaling and similarity arguments of the surface layer, as will be discussed in more detail in a later chapter. It is sometimes called a stability parameter, although its magnitude is not directly related to static nor dynamic stability. Only its sign relates to static stability: negative implies unstable, positive implies statically stable. A better description of ζ is "a surface-layer scaling parameter".

We can write an alternative form for ζ by employing the definition of w_*:

$$\zeta = \frac{z}{L} = -\frac{k\,z\,w_*^3}{z_i\,u_*^3} \tag{5.7d}$$

Fig. 5.22 shows the variation of TKE budget terms with ζ, as ζ varies between 0 (statically neutral) and -1 (slightly unstable). The decrease in importance of shear and increase of buoyancy as ζ decreases from 0 to -1 is particularly obvious.

Fig. 5.22 Behavior of the terms (made dimensionless with kz/u_*^3) in the unstable surface-layer turbulence kinetic energy budget. After Wyngaard (1973).

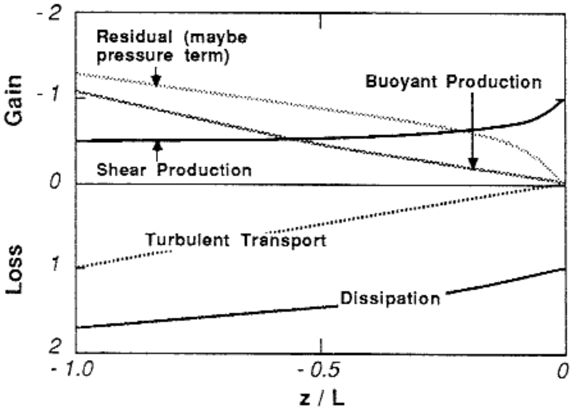

Figs. 5.23 shows the variation of Ri with ζ from slightly unstable to slightly stable conditions. For unstable situations, $Ri \cong \zeta$. One must keep in mind that ζ can be calculated only for turbulent flow, thus this figure shows only the subset of all data that

was turbulent. Nonturbulent flow can occur in stable situations, but it does not appear in this figure.

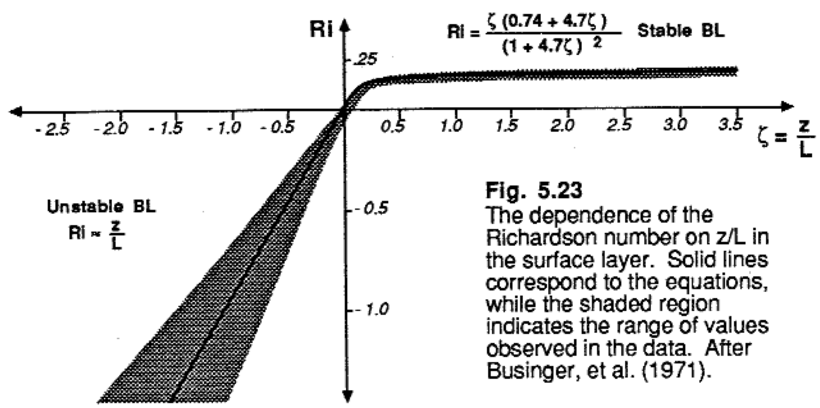

Fig. 5.23
The dependence of the Richardson number on z/L in the surface layer. Solid lines correspond to the equations, while the shaded region indicates the range of values observed in the data. After Businger, et al. (1971).

5.8 Dimensionless Gradients

We can simplify term IV of the dimensionless TKE equation (5.7a) by choosing a coordinate system aligned with the mean wind, assuming horizontal homogeneity, neglecting subsidence, and using the definition that $u_*^2 = -(\overline{u'w'})_s$:

$$\text{Term IV} = \frac{-k\,z}{u_*}\frac{\partial\overline{U}}{\partial z}$$

Based on this dimensionless term, we can define a ***dimensionless wind shear***, ϕ_M, by

$$\phi_M = \frac{k\,z}{u_*}\frac{\partial\overline{U}}{\partial z} \tag{5.8a}$$

This parameter is primarily useful for studies of surface-layer wind profiles and momentum fluxes. In chapter 9 we will use ϕ_M in similarity theory to estimate momentum flux (as given by u_*) from the local mean wind shear. This is particularly valuable because it is easy to measure mean wind speeds at a variety of heights in the surface layer, but much more difficult and expensive to measure the eddy correlations such as $\overline{u'w'}$.

By analogy, a ***dimensionless lapse rate***, ϕ_H, and a ***dimensionless humidity gradient***, ϕ_E , can be defined:

$$\phi_H = \frac{k\,z}{\theta_*^{SL}} \frac{\partial \overline{\theta}}{\partial z} \tag{5.8b}$$

$$\phi_E = \frac{k\,z}{q_*^{SL}} \frac{\partial \overline{q}}{\partial z} \tag{5.8c}$$

These dimensionless gradients are equally as valuable as the dimensionless shear, because using similarity theory we can estimate the surface layer heat flux and moisture flux from simple measurements of lapse rate and moisture gradient, respectively.

5.9 Miscellaneous Scaling Parameters

5.9.1 Definitions

A few additional dimensionless scaling groups have been suggested in the literature to help explain boundary layer characteristics. Again, these are often inappropriately called stability parameters. One parameter that is useful in the surface layer is:

$$\mu^{SL} = \frac{k\,u_*}{f_c\,L} \tag{5.9.1a}$$

$$= \frac{g\,k^2 \overline{(w'\theta_v')}_s}{\overline{\theta_v}\; f_c \overline{(u'w')}_s} \tag{5.9.1b}$$

$$= \frac{g\,k^2\,\theta_*^{SL}}{\overline{\theta_v}\; f_c\,u_*} \tag{5.9.1c}$$

Another scaling parameter that is useful in the ML is

$$\mu^{ML} = k\,\frac{z_i}{L} \tag{5.9.1d}$$

$$= \frac{-k^2 \left(\frac{g}{\overline{\theta_v}}\right) \overline{(w'\theta_v')}_s}{u_*^3} \tag{5.9.1e}$$

$$= -k^2 \frac{w_*^3}{u_*^3} \qquad (5.9.1f)$$

It's important not to confuse either of these two parameters with the dynamic viscosity, which traditionally uses the same symbol.

Another parameter occasionally used is:

$$s_G = \frac{\overline{\theta}_s - \overline{\theta}_{air}}{\overline{M}^2 \left[1 + \log\left(\frac{10}{z} \right) \right]^2} \qquad (5.9.1g)$$

which looks like a modified Richardson number. Additional scaling parameters and dimensionless groups will be introduced in later chapters where appropriate.

5.9.2 Example

Problem: Given surface measurements: $u_* = 0.2\ \text{m·s}^{-1}$, $g/\overline{\theta_v} = 0.0333\ \text{m·s}^{-1}\text{K}^{-1}$, and $\overline{w'\theta_v'} = -0.05\ \text{K·m·s}^{-1}$; and at 10 m: $\partial\overline{U}/\partial z = 20\ \text{m·s}^{-1}/100\text{m}$, and $\partial\overline{\theta_v}/\partial z = 20\ ^\circ\text{C}/100\text{m}$. Find scaling parameters L, ζ, θ_*^{SL}, ϕ_M, ϕ_H, and μ^{SL} at z = 10 m, at a latitude where $f_c = 10^{-4}\ \text{s}^{-1}$.

Solution: $$L = \frac{-u_*^3}{k\,(g/\overline{\theta_v})\,\overline{w'\theta_v'}} = \frac{(0.2)^3}{(0.4)\,(0.0333)\,(0.05)} = 12.0\ \text{m}$$

$$\zeta = \frac{z}{L} = \frac{10}{12} = 0.83$$

$$\phi_M = \frac{k\,z}{u_*}\frac{\partial\overline{U}}{\partial z} = \frac{(0.4)\,(10)}{(0.2)}(0.2) = 4.0$$

$$\theta_*^{SL} = \frac{-\overline{w'\theta_v'}_s}{u_*} = \frac{0.05}{0.2} = 0.25\ \text{K}$$

$$\phi_H = \frac{k\,z}{\theta_*^{SL}} \frac{\partial \overline{\theta_v}}{\partial z} = \frac{(0.4)\,(10)}{(0.25)}\,(0.2) = 3.2$$

$$\mu^{SL} = \frac{k\,u_*}{f_c\,L} = \frac{(0.4)\,(0.2)}{(10^{-4})\,(12)} = 66.7$$

5.10 Combined Stability Tables

Static and dynamic stability concepts are intertwined, as sketched in Fig 5.24a. Negative Richardson numbers always correspond to statically and dynamically unstable flow. This flow will definitely become turbulent. Positive Richardson numbers are always statically stable, but there is the small range of $0 < Ri < 1$ where positive Richardson numbers are dynamically unstable, and may be turbulent depending on the past history of the flow. Namely, nonturbulent flow will become turbulent at about $Ri = 0.25$, while flow that is presently turbulent will stay turbulent if $Ri < 1$.

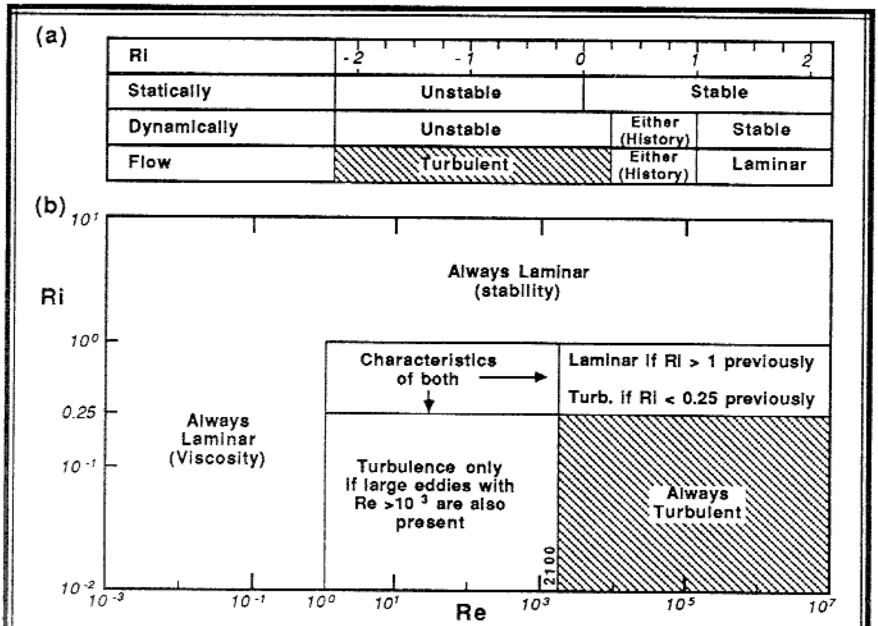

Fig. 5.24 Stability parameter relationships (see text). (After Woods, 1969).

The effects of viscosity and stability in suppressing turbulence are also intertwined, as sketched in Fig 5.24b. In Section 3.5.1 we defined the Reynolds number as the ratio of inertial to viscous forces, with no mention about buoyancy. In section 5.5.3, we defined a Richardson number as the ratio of buoyant to inertial or mechanical forces, with no mention of viscosity. In the atmosphere, the Reynolds number is usually so large that it corresponds to the rightmost edge of Fig 5.24b. Thus, we can essentially ignore viscous effects on stability in the atmosphere, and focus on the static and dynamic stability instead.

In conclusion, we see that the TKE equation is critical for determining the nature of flow in the BL. The relative contributions of various turbulence production and loss terms can be compared when rewritten as dimensionless scaling parameters. These parameters can be used to define layers within the BL where the physics is simplified, and where a variety of similarity scaling arguments can be made (see chapter 9 for details of similarity theory).

5.11 References

André, J.-C., G. De Moor, P. Lacarrère, G. Therry, and R. du Vachat, 1978: Modeling the 24-hour evolution of the mean and turbulent structures of the planetary boundary layer. *J. Atmos. Sci.*, **35**, 1861-1883.

Businger, J.A., J.C. Wyngaard, Y. Izumi and E.F. Bradley, 1971: Flux profile relationships in the atmospheric surface layer. *J. Atmos. Sci.*, **28**, 181-189.

Caughey, S.J., J.C. Wyngaard and J.C. Kaimal, 1979: Turbulence in the evolving stable boundary layer. *J. Atmos. Sci.*, **36**, 1041-1052.

Chou, S.-H., D. Atlas, and E.-N. Yeh, 1986: Turbulence in a convective marine atmospheric boundary layer. *J. Atmos. Sci.*, **43**, 547-564.

Deardorff, J.W., 1974: Three-dimensional numerical study of turbulence in an entraining mixed layer. *Bound.-Layer Meteor.*, **7**, 199-226.

Gal-Chen, T. and R.A. Kropfli, 1984: Buoyancy and pressure perturbations derived from dual-Doppler radar observations of the planetary boundary layer: applications for matching models with observations. *J. Atmos. Sci.*, **41**, 3007-3020.

Hechtel, L.M., 1988: The effects of nonhomogeneous surface heat and moisture fluxes on the convective boundary layer. *Preprints of the Am. Meteor. Soc. 8th Symposium on Turbulence and Diffusion in San Diego, April 1988.* 4pp.

Holtslag, A.A.M. and F.T.M. Nieuwstadt, 1986: Scaling the atmospheric boundary layer. *Bound.-Layer Meteor.*, **36**, 201-209.

Kitchen, M., J.R. Leighton and S.J. Caughey, 1983: Three case studies of shallow convection using a tethered balloon. *Bound.-Layer Meteor.*, **27**, 281-308.

Lee, D.R., R. B. Stull, and W.S. Irvine, 1979: *Clear Air Turbulence Forecasting Techniques*. AFGWC/TN-79/001. Air Force Global Weather Central, Offutt AFB, NE 68113. 73pp.

Lenschow, D.H., 1974: Model of the height variation of the turbulence kinetic energy budget in the unstable planetary boundary layer. *J. Atmos. Sci.*, **31**, 465-474.

Lenschow, D.H., J.C. Wyngaard and W.T Pennell, 1980: Mean field and second moment budgets in a baroclinic, convective boundary layer. *J. Atmos. Sci.*, **37**, 1313-1326.

Louis, J.F., A. Weill and D. Vidal-Madjar, 1983: Dissipation length in stable layers. *Bound.-Layer Meteor.*, **25**, 229-243.

Mahrt, L., 1981: Modelling the depth of the stable boundary layer. *Bound.-Layer Meteor.*, **21**, 3-19.

McBean, G.A. and J.A. Elliott, 1975: The vertical transports of kinetic energy by turbulence and pressure in the boundary layer. *J.Atmos. Sci.*, **32**, 753-766.

Nicholls, S., M.A. LeMone and G. Sommeria, 1982: The simulation of a fair weather marine boundary layer in GATE using a three dimensional model. *Quart. J. Roy. Meteor. Soc.*, **108**, 167-190.

Nicholls, S. and C.J. Readings, 1979: Aircraft observations of the structure of the lower boundary layer over the sea. *Quart. J. Roy. Meteor. Soc.*, **105**, 785-802.

Noonkester, V.R., 1974: Convective activity observed by FM-CW radar. Naval Electronics Lab. Center, NELC/TR 1919. San Diego, CA 92152. 70pp.

Pennell, W.T. and M.A. LeMone, 1974: An experimental study of turbulence structure in the fair-weather trade wind boundary layer. *J. Atmos. Sci.*, **31**, 1308-1323.

Stage, S.A. and J.A. Businger, 1981: A model for entrainment into a cloud-topped marine boundary layer. Part I. Model description and application to a cold air outbreak episode. *J. Atmos. Sci.*, **38**, 2213-2229.

Therry, G. and P. Lacarrère, 1983: Improving the eddy kinetic energy model for planetary boundary layer description. *Bound.-Layer Meteor.*, **25**, 63-88.

Thorpe, S.A., 1969: Experiments on the stability of stratified shear flows. *Radio Science*, **4**, 1327-1331.

Thorpe, S.A., 1973: CAT in the lab. *Weather*, **28**, 471-475.

Wilczak, J.M. and J.A. Businger, 1984: Large-scale eddies in the unstably stratified atmospheric surface layer. Part II. Turbulent pressure fluctuations and the budgets of heat flux, stress and turbulent kinetic energy. *J. Atmos. Sci.*, **41**, 3551-3567.

Woods, J.D., 1969: On Richardson's number as a criterion for laminar-turbulent-laminar transition in the ocean and atmosphere. *Radio Science*, **4**, 1289-1298.

Wyngaard, J.C., 1973: On surface layer turbulence. *Workshop on Micrometeorology*, D.A. Haugen (Ed.), Amer. Meteor. Soc., Boston. 101-149.

Yamada, T. and G. Mellor, 1975: A simulation of the Wangara atmospheric boundary layer data. *J. Atmos. Sci.*, **32**, 2309-2329.

Zhou, M.Y., D.H. Lenschow, B.B. Stankov, J.C. Kaimal, and J.E. Gaynor, 1985: Wave and turbulence structure in a shallow baroclinic convective boundary layer and overlying inversion. *J. Atmos. Sci.*, **42**, 47-57.

5.12 Exercises

1) Why doesn't turbulent energy cascade from small to large eddies (or wavelengths) in the boundary layer?
2) Refer to the TKE equation. Which term(s), if any, represent the production of turbulence during a day when there are light winds and strong solar heating of the boundary layer?
3) Given the following wind speeds measured at various heights in the boundary layer:

z (m)	U (m/s)
2000	10.0
1000	10.0
500	9.5
300	9.0
100	8.0
50	7.4
20	6.5
10	5.8
4	5.0
1	3.7

Assume that the potential temperature increases with height at the constant rate of 6 K/km. Calculate the bulk Richardson number for each layer and indicate the static and dynamic stability of each layer. Also, show what part of the atmosphere is expected to be turbulent in these conditions.

4) Derive an expression for the kinematic heat flux $\overline{w'\theta'}$ in terms of the dimensionless wind shear ϕ_M and dimensionless lapse rate ϕ_H.
5) Given the following TKE equation:

$$\underset{A}{\frac{\partial \bar{e}}{\partial t}} + \underset{B}{\overline{U}_j \frac{\partial \bar{e}}{\partial x_j}} = \underset{C}{-\overline{u'w'}\frac{\partial \overline{U}}{\partial z}} + \underset{D}{\frac{g}{\overline{\theta}_v}\left(\overline{w'\theta_v'}\right)} - \underset{E}{\frac{\partial\left(\overline{w'e}\right)}{\partial z}} - \underset{F}{\frac{1}{\overline{\rho}}\frac{\partial\left(\overline{w'p'}\right)}{\partial z}} - \underset{G}{\varepsilon}$$

a. Which terms are always loss terms?
b. Which terms neither create nor destroy TKE?
c. Which terms can be either production or loss?
d. Which terms are due to molecular effects?
e. Which production terms are largest on a cloudy, windy day?
f. Which production terms are largest on a calm sunny day over land?
g. Which terms tend to make turbulence more homogeneous?
h. Which terms tend to make turbulence less isotropic?
i. Which terms describe the stationarity of the turbulence?
j. Which terms describe the kinetic energy lost from the mean wind?

6) Very briefly define the following, and comment or give examples of their use in micrometeorology.

a. inertial subrange
b. friction velocity
c. Obukhov length
d. return-to-isotropy term
e. static stability
f. convective velocity scale
g. Reynold's stress
h. turbulence closure problem
i. Richardson number
j. TKE

7) Fill in the table based on the regions A-H labeled on the attached diagram.

Property:	**Lapse Rate**	**Heat Flux**	**Static Stability**	**Turbulent?**	**Name**
Choices:	Subadiab. Adiabatic Superad.	Up Zero Down	Stable Neutral Unstable	Yes Unknown No Sporadic	Noct. inversion Cloud layer Mixed layer Entrainment Zone Capping inversion Free atmosphere
Region					
A					Surface layer
B					
C	Subadiab.				
D					
E					Residual layer
F		Zero			
G				Unknown	
H			Stable		

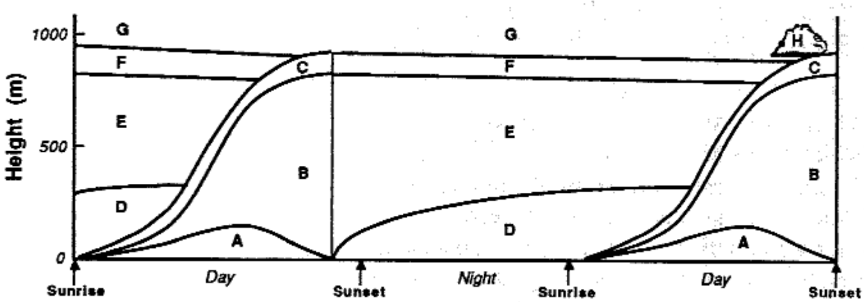

8) It has been suggested that in regions of strong static stability, the lower end of the inertial subrange (long wavelength, small wavenumber) occurs at a wavenumber, κ_b, given by: $\kappa_b \cong N_{BV}^{3/2}\ \varepsilon^{-1/2}$, where N_{BV} is the Brunt-Väisäla frequency, and ε is the TKE dissipation rate. Within the buoyancy subrange sketched below, would you expect turbulence to be isotropic? (Hint, buoyancy effects are important in a statically stable environment.)

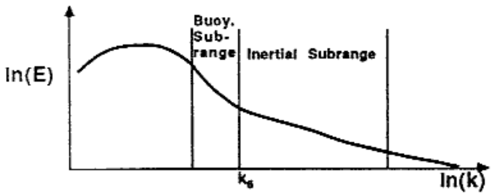

9) a) Rewrite the conservation equation for mean kinetic energy in terms of the geostrophic wind.

b) Suppose that $\overline{u'w'} = -0.05\ m^2\ s^{-2}$ and $\partial\overline{U}/\partial z = 5\ s^{-1}$ and $\overline{V} = 0$ within the surface layer. If there are no pressure gradients, then what is the value of the rate of change of mean kinetic energy, and what does it mean concerning the change in mean wind speed during a 1 minute period?

10) On the planet Krypton suppose that turbulent motions are affected by a strange form of viscosity that dissipates only the vertical motions. How would the TKE be affected?

11) What is the Reynolds stress? Why is it called a stress? How does it relate to u_*?

12) Define the following types of convection. Under what weather conditions is each type of convection most likely? What term in the TKE equation is small under each condition?

a) Free convection

b) Forced convection.

13) Given the term: $U_j\ \partial(\frac{1}{2}V^2)/\partial x_j$, which represent the advection of total horizontal v-component of kinetic energy. Expand the variables U_j and V into mean and turbulent parts, Reynolds average, and simplify as much as possible.

14) Observations:

z(m):	12	8	2	$0.1 = z_o$
$\overline{\theta}$ (K):	300	301	303	308
$\overline{U}$(m/s)	5.4	5.0	3.4	0

Situation: Daytime boundary layer over land.

a) Find R_B at 2, 4, and 10m.

b) Comment on the static and dynamic stability of the air. Is the flow turbulent?

15) If the TKE at 10m is at steady state, and if $\varepsilon = 0.01\ m^2\ s^{-3}$, then is the transport term supplying or removing TKE from the air at z = 10m?

16) What is the static stability of each of the layers in the diagram at right?

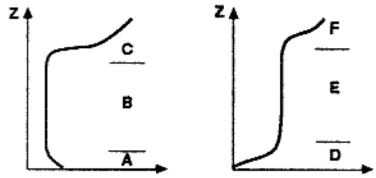

17) This problem is best saved until after the log-wind profile has been introduced. Given the following data:

$\overline{w'\theta'} = 0.2$ K m/s	$u_* = 0.2$ m/s
$z_i = 500$ m	$k = 0.4$
$g/\overline{\theta} = 0.0333\ m\ s^{-2}\ K^{-1}$	$z = 6$ m
$z_o = 0.01$ m = roughness length	no moisture

Find:

a) L	f) R_f at 6m (make assumptions to find this)
b) z/L	g) Ri at 6m (make assumptions to find this)
c) w_*	h) dynamic stability
d) θ_*	i) flow state (turbulent or not)
e) static stability	

18) Given the following sounding in the morning boundary layer. Determine whether each layer is stable or unstable (in both the static and dynamic sense), and state if the flow is turbulent. Indicate your results in the table to the right of the figures.

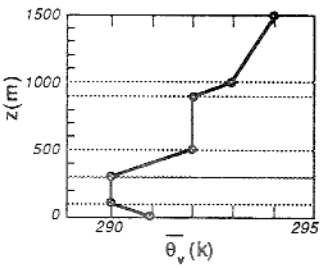

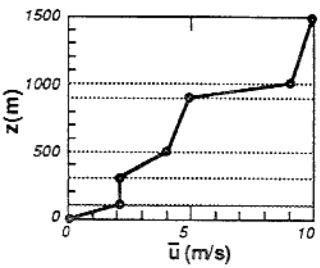

Ri	Static	Dynam.	Turb.

19) Given the following turbulence statistics.

Where:	Location A		Location B	
When (UTC):	1000	1100	1000	1100
Statistic				
$\overline{u'^2}$ ($m^2\ s^{-2}$)	0.50	0.50	0.70	0.50
$\overline{v'^2}$ ($m^2\ s^{-2}$)	0.25	0.50	0.25	0.25
$\overline{w'^2}$ ($m^2\ s^{-2}$)	0.70	0.50	0.70	0.25

Where and when is the turbulence
a) Stationary b) Homogeneous c) Isotropic?

20) What boundary layer flow phenomena or characteristics have scale sizes on the order of: a) 1 mm, b) 10 m, c) 1 km ?

21) Fill in the blanks in the table below:

Characteristic: / **Phenomenon:**	**Convective turbulence in the BL**	**Mechanical turbulence in the BL**
• Name of (or symbol for) a characteristic depth scale:		
• Name of (or symbol for) a characteristic velocity scale:		
• Name of the type of convection associated with this phenomenon:		
• Dominant production term in the TKE equation:		
• Sign of the gradient Richardson number:		
• Direction (horizontal or vertical) of the dominant anisotropic component of turbulence:		

22) a) Is θ_v conserved during adiabatic ascent of an unsaturated air parcel? If not, does it increase or decrease with height?
b) Same question, but in saturated (cloudy) air.
c) If a saturated air parcel at 80 kPa (800 mb) has $T = 4$ °C (thus, $r_s = 6.5$ g/kg) and has a total water mixing ratio of $r_T = 8.0$ g/kg, then calculate the virtual potential temperature at that altitude.

23) Given the TKE equation with terms labeled A to E below:

$$\frac{\partial \bar{e}}{\partial t} = -\overline{u'w'}\frac{\partial \overline{U}}{\partial z} + \frac{g}{\overline{\theta_v}}\overline{w'\theta_v'} - \frac{\partial}{\partial z}\overline{w'\left(\frac{p'}{\overline{\rho}} + e\right)} - \varepsilon$$

A B C D E

and given 4 regions of the stable boundary layer, labeled I to IV in the figure below, determine the sign (+ , - , or near zero) of each term in each region. (Assume: that term A is always zero; i.e., steady state.)

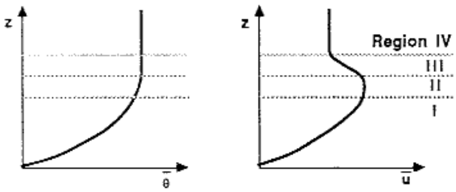

24) The dissipation rate of TKE is sometimes approximated by $\varepsilon = \bar{e}^{3/2} / l$, where l is the ***dissipation length scale***. It is often assumed that $l = 5$ z in statically neutral conditions (Louis, et al., 1983). If the TKE shown in Fig 2.9b is assumed as an initial condition, there is no shear or buoyancy production or loss, and no redistribution nor turbulent transport, then at z = 100m:

a) What is the initial value of the dissipation rate?

b) How long will it take the TKE to decay to 10% of its initial value?

25) Given $\overline{w'\theta_v'} = 0.3$ K m/s, $\overline{u'w'} = -0.25$ m^2 s^{-2}, and $z_i = 1$ km, find:

a) u_*

b) w_*

c) t_*^{ML}

d) θ_*^{ML}

e) θ_*^{SL}

f) R_f (assume $\partial U/\partial z = 0.1$ s^{-1})

g) Obukhov length (L)

26) Given the following sounding, indicate for each layer the

a) static stability

b) dynamic stability

c) existence of turbulence (assuming a laminar past history).

z (m)	$\overline{\theta_v}$ (K)	$\overline{U}$ (m/s)
80	305	18
70	305	17
60	301	15
50	300	14
40	298	10
30	294	8
20	292	7
10	292	7
0	293	2

27) Which Richardson number (flux, gradient, bulk) would you use for the following application? (Give the one best answer for each question).
 a) Diagnose the possible existence of clear air turbulence using rawinsonde data.
 b) Determine whether turbulent flow will become laminar.
 c) Determine whether laminar flow will become turbulent in the boundary layer.

28) What is the difference between free and forced convection?

29) What is the Reynolds number? Of what importance is it to boundary layer flows?

30) What is the closure problem?

31) Given isotropic turbulence with $u_* = 0.5$ m/s and TKE/m = 0.9 $m^2\ s^{-2}$, find the correlation coefficient, r, between w and u.

32) Given the TKE equation, name each term and describe how you could determine the value of each term.

33) Indicate the nature of the flow (laminar or turbulent) for each cell in the table below: